EG&G Idaho, Inc.

FORM EG&G-396
(Rev. 11-79)

INTERIM REPORT

Accession No. _____

Report No. ECC-CAAD-5375

Contract Program or Project Title: Code Assessment and Applications Division

Subject of this Document: RELAP4/MOD7 Modeling Sensitivity Studies for Small Break Transients

Type of Document: Preliminary Assessment Report

Author(s): C. A. Dobbe

NRC Research and Technical Assistance Report

Date of Document: March 1981

Responsible NRC Individual and NRC Office or Division: F. Odar, NRC-RSR, J. Guttmann, NRC-NRR

This document was prepared primarily for preliminary or internal use. It has not received full review and approval. Since there may be substantive changes, this document should not be considered final.

EG&G Idaho, Inc.
Idaho Falls, Idaho 83415

Prepared for the
U.S. Nuclear Regulatory Commission
Washington, D.C.
Under DOE Contract No. DE-AC07-76ID01570
NRC FIN No. A6047

INTERIM REPORT

ABSTRACT

Sensitivity studies for small break calculations, using a model of the Westinghouse Zion I pressurized water reactor, were performed with an experimental version of the RELAP4/MOD7 computer code. Calculations were performed to evaluate the sensitivity of the results of a 0.1016 m diameter cold leg break calculation to downcomer noding, cold leg modeling, circumferential break location, and the RELAP4/MOD7 nonequilibrium model.

SUMMARY

A series of thirteen RELAP4/MOD7 small break calculations were performed to study the sensitivity of the results to nodalization changes and modeling options. The small break model used for the sensitivity studies was a 0.1016 m diameter cold leg break in the Zion I pressurized water reactor.

Two calculations were performed to determine a reference calculation for the study. A best estimate calculation and an evaluation model calculation were performed with calculated core uncovery being the primary selection criteria. The evaluation model was selected as the reference calculation.

Four calculations were performed to evaluate the sensitivity of the reference calculation results to downcomer nodalization. Simple and detailed nodalizations were examined for modeling the downcomer inlet annulus and downcomer regions. A recommendation for downcomer noding was not obtained due to problems related to the RELAP4/MOD7 mixture level crossing model. The mixture level crossing model would not allow the mixture level to drop below the junction connecting the inlet annulus to the downcomer.

Four additional calculations were performed to assess the sensitivity of the reference calculation results to modeling phase separation in the cold leg and varying the circumferential location of the break about the cold leg. Due to the aforementioned problems with the mixture level crossing model and lack of a suitable horizontal slip model in RELAP4/MOD7 there were no recommendations made for modeling of phase separation in the cold legs. The circumferential break location study indicated that the calculated results were insensitive to break location.

Three calculations were performed to evaluate the effect of the RELAP4/MOD7 nonequilibrium model on both the reference calculation and on the calculation with phase separation in the cold legs. The nonequilibrium

model alleviated the calculated unrealistic pressure drop following accumulator initiation that occurs in calculations with equilibrium assumed. The interaction between the nonequilibrium model, mixture level crossing model, and Wilson bubble rise model need to be assesed further.

CONTENTS

ABSTRACT ii

SUMMARY iii

1. INTRODUCTION 1

2. MODEL DESCRIPTION 3

2.1 Code Description 3

2.2 Nodalizations 3

2.3 Code Options 3

2.4 Boundary and Initial Conditions 5

3. CALCULATED RESULTS 10

3.1 Base Case 10

3.2 Downcomer Noding Study 11

3.3 Cold Leg Modeling Study 16

3.4 Break Circumferential Location Study 18

3.5 Nonequilibrium Modeling Study 19

4. CONCLUSIONS AND RECOMMENDATIONS 22

5. REFERENCES 23

APPENDIX-A--METRIC TO ENGLISH CONVERSION FACTORS 24

FIGURES

1. Nodalization for Run A-1 32

2. Nodalization for Run B-1 33

3. Nodalization for Runs A-2, C, D-1, D-2, D-3, E-1, E-2, and E-3 34

4. Nodalization for Run B-2 35

5. Nodalization for Run B-3 36

6. Nodalization for Run B-4 37

7. Upper plenum pressure vs. time for Runs A-1 and A-2 38

8. Steam generator secondary side pressure vs. time for Runs A-1 and A-2 38

9. Upper plenum and core volume mixture levels vs. time for Runs A-1 and A-2 39

10. Fuel rod cladding surface temperature 3.0-3.7 m above the core inlet vs. time for Runs A-1 and A-2 39

11. Downcomer and downcomer inlet annulus mixture levels vs. time for Runs A-1 and B-1 40

12. Upper plenum pressure vs. time for Runs A-1 and B-1 40

13. Integrated broken loop accumulator mass flow vs. time for Runs A-1 and B-1 41

14. Upper plenum pressure vs. time for Runs A-2 and B-2 41

15. Downcomer and downcomer inlet annulus mixture levels vs. time for Runs A-2 and B-2 42

16. Upper plenum and core mixture levels vs. time for Runs A-2 and B-2 42

17. Fuel rod cladding surface temperature 3.0-3.7 m above the core inlet vs. time for Runs A-2 and B-2 43

18. Upper plenum pressure vs. time for Runs A-2, B-3, and B-4 43

19. Downcomer and downcomer inlet annulus mixture levels vs. time for Runs A-2, B-3 and B-4 44

20. Upper plenum and core mixture levels vs. time for Runs A-2, B-3 and B-4 44

21. F el rod cladding surface temperature 3.0-3.7 m above the core inlet vs. time for Runs A-2, B-3 and B-4 45

22. Broken loop cold leg mixture level vs. time for Run C 45

23. Break mass flow rate vs. time for Runs A-2 and C 46

24. Downcomer and downcomer inlet annulus mixture levels vs. time for Runs A-2 and C 46

25. Broken loop cold leg mixture level vs. time for Runs C, D-1, and D-3 47

26. Integrated broken loop accumulator mass flow vs. time for Runs C, D-1, and D-3 47

27. Upper plenum pressure vs. time for Runs C, D-1, and D-3 48

28. Upper plenum pressure vs. time for Runs A-2 and E-1 48

29. Integrated broken loop accumulator mass flow vs. time for Runs A-2 and E-1 49

30. Upper plenum and core mixture levels vs. time for Runs A-2 and E-1 49

31. Fuel rod cladding surface temperature 3.0-3.7 m above the core inlet vs time for Runs A-2 and E-1 50

32. Upper plenum pressure vs. time for Runs C, E-2 and E-3 50

33. Broken loop cold leg mixture level vs. time for Runs C, E-2, and E-3 51

34. Integrated broken loop accumulator mass flow vs. time for Runs C, E-2, and E-3 51

35. Upper plenum and core mixture levels vs. time for Runs C, E-2, and E-3 .....

36. Fuel rod cladding surface temperature 3.0-3.7 m above the core inlet vs. time for Runs C, E-2, and E-3 .....

TABLES

1. Sensitivity Calculation Matrix 26

2. Safety Injection Flow Rate as a Function of Primary System Pressure--Best Estimate 27

3. Charging Flow Rate as a Function of Primary System Pressure--Best Estimate 28

4. Steam Generator Secondary Dump and Safety Valve Flow Rate as a Function of Secondary System Pressure--Best Estimate 28

5. Safety Injection Flow Rate as a Function of Primary System Pressure-Evaluation Model 29

6. Description of Input Decks Used for RELAP4/MOD7 Sensitivity Studies 30

7. Computer Run Times for the RELAP4/MOD7 Sensitivity Studies 31

1. INTRODUCTION

The RELAP4/MOD7[1] computer code was developed to investigate the thermal-hydraulic response of a nuclear reactor or related system under normal or accident conditions. The emphasis during development and checkout of the RELAP4/MOD7 computer code was toward integral calculations of blowdown, refill, and reflood during postulated large area pipe breaks. Code sensitivity to various modeling and analytical techniques during small break transients was not rigorously assessed. The purpose of this report is to document the results of a series of calculations which were performed to evaluate the sensitivity of RELAP4/MOD7 calculated results for selected modeling techniques for a postulated small cold leg break transient.

The calculations performed for the study, referenced by an index letter and number, are grouped into five categories as shown in Table 1. Each calculation assumed a 0.1016 m diameter break in one of the Zion I reactor cold legs. The modeling techniques and assumptions used for the study are described in Section 2. The calculational results are discussed in Section 3 and conclusions and recommendations are presented in Section 4.

The category A calculations were performed to evalute both best estimate and evalution model (licensing) accident analyses. One calculation was selected as a reference calculation for the study.

The category B calculations were performed to determine the sensitivity of the results to changes in the number of nodes representing the downcomer inlet annulus and downcomer regions.

Category C consisted of a single calculation performed to evaluate the effect of modeling phase separation in the cold legs on the results of the reference calculation.

Category D calculations evaluated the effects of the break circumferential location on the broken loop cold leg pipe to determine if the results of the category C calculation were sensitive to break location.

Three calculations were performed for category E to determine the effect of the RELAP4/MOD7 nonequilibrium model on a calculation with homogeneous assumptions used in the cold legs and a calculation with phase separation in the cold legs. These are Runs E-1 and E-2, respectively. Run E-3 was performed to evaluate the sensitivity of the interphase heat transfer multiplier (user input) on the Run E-2 calculation. The nonequilibrium model was tripped on at 930 s in all category E calculations.

2. MODEL DESCRIPTION

The nodalization schemes used in the sensitivity studies are based on RELAP4 models developed during the BE/EM Study.[1] The original BE/EM models were revised and modified in subsequent tasks (References 2 and 3) resulting in "best-estimate" and "licensing" (evaluation model) input decks. These input decks were the starting point for this study. A description of the nodalizations, code description, code options, and boundary and initial conditions used for the sensitivity studies are presented in the following section.

2.1 Code Description

The RELAP4/MOD7 computer code was used to perform the sensitivity studies. The version used was the released version stored at the Idaho National Engineering Laboratory (INEL) under Configuration Control Numbers H01345IB (RELAP4/MOD7) and H009982B (steam tables). The code was updated during restarts to set the boundary input tape flag to false.

2.2 Nodalizations

The nodalization schemes are shown in Figures 1 through 6. The nodalizations differ in downcomer inlet annulus modeling, downcomer modeling and in the volume and junction numbering. The numbering changes were necessary due to the RELAP4/MOD7 self initialization routine requirement of contiguous volume and junction numbering. The nodalizations shown in Figures 1 and 2 are derived from Reference 1 with the remaining nodalizations based on the model documented in Reference 2.

2.3 Code Options

The following user selected options were used for the sensitivity studies.

1. A MVMIX value of 0 (compressible flow with momentum flux) was used at all junctions, except that a MVMIX value of 3 (incompressible flow with no momentum flux) was used at junctions between the vessel and hot and cold legs, pressurizer and accumulator junctions with the primary piping, core bypass and all fill junctions.

2. The Wilson bubble rise model was used in the inlet annulus, downcomer, lower plenum, upper plenum and head, pressurizer, and pump suction volumes for all calculations. The Wilson bubble rise was also used in all cold leg volumes between the pumps and the vessel for Runs C, D-1, D-2, D-3, E-2 and E-3. A bubble gradient of 0.8 was used for all calculations.

3. Complete phase separation was modeled in the accumulator volumes.

4. A constant bubble rise velocity and bubble gradient were used in the steam generator secondaries. The values were calculated by the code to achieve an initial energy balance.

5. Core heat transfer was calculated with the default and/or recommended options for the RELAP4/MOD6 Update 4 computer code. These options include (a) use of HTS2 heat transfer surface, (b) CHF calculated with recommended CHF correlations, (c) transition boiling calculated with modified Tong-Young correlation, and (d) film boiling calculated with the Condie-Bengston III film boiling correlation. The recommended CHF correlations are the W-3 correlation for the subcooled regime, Hsu and Beckner's modified W-3 correlation for saturated high flow and Smith and Griffith's modified Zuber for the saturated low flow regime.

5. The enthalpy transport model was used to initialize the calculation but was not used during the transient.

6. The RELAP4/MOD7 self-initialization routine was used to effect an initial system pressure and energy balance.

7. A reactor coolant pump bearing friction equal to 2-1/2 percent of rated torque was used.

8. The vertical slip model was used at junctions between the inlet annulus and downcomer, downcomer and lower plenum, lower plenum and core, between core volumes, and between core and upper plenum volumes.

9. The natural convection option for heat transfer was used in the steam generator secondaries.

10. The elevation of the break junction was assumed to have a point value with respect to bubble distribution in the cold leg volume with the junction enthalpy smoothed when the two-phase mixture was near the junction elevation in all runs except Run C. (Note that this option is only significant when phase separation is modeled in the cold legs). For Run C the junction flow area was assumed to be a circular area centered and distributed vertically about the input elevation, ZJUN.

2.4 Boundary and Initial Conditions

The following boundary and initial conditions were used for Runs A-1 and B-1. These correspond exactly to those given in Reference 1.

1. The Normalized Core Axial Power Profile was

Top of Core
0.0397 (core heat slab 6)
0.1791 (core heat slab 5)
0.2122 (core heat slab 4)
0.2139 (core heat slab 3)
0.2101 (core heat slab 2)
0.1450 (core heat slab 1)
Bottom of Core

2. The system initial operating conditions were:

Core Power	:	3238 MW
Hot Leg Temperature	:	582 K
Cold Leg Temperature	:	550 K
S.G. Secondary Pressure	:	5.19 MPa
Upper Plenum Pressure	:	15.6 MPa
Mass Flow Rate Per Loop	:	4606 Kg/s
Feed/Steam Flow Rate Per Loop	:	444.7 Kg/s
Feedwater Enthalpy	:	1016.5 KJ/Kg
Pressurizer Liquid Mass	:	19688 Kg
Pump Speed	:	123.6 rad/s

3. The new ANS decay heat rate was used (Proposed 1977 Standard).

4. Safety injection (SI) flow rate was a function of pressure and the values used are shown in Table 2. These flow rates represent the total output of two HPIS and two LPIS pumps.

5. Charging flow rate was a function of pressure and the values used are shown in Table 3. These flow rates represent the total output of two charging pumps.

6. The steam generator secondary atmospheric dump valve and bank of five code safety valves were modeled by a single negative fill junction. The combined flow rate was dependent on the secondary system pressure and the values used are shown in Table 4.

7. Motor-driven auxiliary feedwater flow was controlled to be fully off when the secondary level exceeded 13.1 m and fully on when the level was lower than 13.1 m. There were two motor driven auxiliary feedwater pumps providing a total flow rate of 14.08 Kg/s to each steam generator. Turbine-driven auxiliary feedwater was provided by a single pump with the same capacity as the combined motor driven pumps and was controlled in the same manner. Auxiliary feedwater enthalpy for both motor and turbine-driven systems was 158.2 KJ/Kg.

8. The Accumulator Inital Conditions were:
   Pressure: 4.14 MPa
   Temperature: 325 K
   Water Volume: 23.2 m^3 per accumulator

9. The three pressurizer code safety valves and two power operated relief valves were modeled by a single negative fill. The combined valves were closed at pressures below 16.89 MPa, passed 52.9[illegible] Kg/s between 16.89 MPa and 17.24 MPa, and passed as much mass as needed above 17.24 MPa to prevent a further pressure increase. These valves were not challenged in any of the calculations.

10. A primary leakage rate of 0.6308 l/s was used for all the calculations.

11. Reactor coolant primary loop heat loss to containment was not modeled. This heat loss was estimated to be 0.95 Mw which was less than 2% of the decay heat rate.

12. Scram occurred 3.4 seconds after the scram signal was received due to a low pressurizer pressure of 12.62 MPa. The reactor coolant pumps were tripped off upon reactor scram.

13. The safety injection (SI) signal was generated when the pressurizer pressure decreased below 12.62 MPa. SI and charging flows were automatically initiated after a 5 second delay from the SI signal.

For Runs A-2, B-2, B-3, B-4, and all category C, D, and E runs, the following initial conditions (taken from Reference 2) were used.

1. The normalized core axial power profile used was:

Top of Core

0.167 (core heat slab 6)
0.222 (core heat slab 5)
0.184 (core heat slab 4)
0.157 (core heat slab 3)
0.148 (core heat slab 2)
0.122 (core heat slab 1)

Bottom of Core

2. The decay heat used was ANS + 20 percent (Proposed 1977 Standard)

3. The safety injection flow dependence on primary system pressure which assumed one HPI pump was operating is given in Table 5. Safety injection was tripped on 25 seconds after the pressurizer pressure decreased to 1.21 MPa.

4. Steam generator safety valve full rated flow (FRF) was 523.2 kg/s per steam generator. The valve opened at 820 kPa allowing 8 percent FRF to pass and the flow rate increased linearly to 100 percent FRF at 862 kPa.

5. The full rated feedwater flow was 508.1 kg/s per steam generator. Feedwater flow remained at full flow until 5 seconds after scram and remained at 0 until 59 seconds after SCRAM. Auxiliary feedwater flow was turned on linearly from 59 to 60 seconds after scram and remained on at 1.928% of the full flow. The main feedwater enthalpy was 973.7 KJ/kg and the auxiliary feedwater enthalpy was 211.7 KJ/kg.

6. The Accumulator Initial Conditions were:
   P = 4.14 MPa
   T = 325 K
   Water Volume = 23.2 m^3 per accumulator

7. Scram occurred 3.4 seconds after the scram signal was received due to a pressurizer pressure decrease to 1.28 MPa. The reactor coolant pumps were tripped off upon reactor scram.

8. Pressurizer initial mass was 21823 Kg of which 2136 kg was vapor.

9. A turbine trip coincident with scram signal closed the steam generator outlet valves.

10. The system operating conditions were:

Mass Flow Rate per Loop	:	4419 Kg/s
Upper Plenum Pressure	:	15.76 MPa
S. G. Secondary Pressure	:	6.89 MPa
Cold Leg Temperature	:	569.1 K
Hot Leg Temperature	:	603.8 K
Core Power	:	3649 MW

The JCL and input decks used for the sensitivity studies are stored at the INEL under Configuration Control Number F00065. The decks are stored in a sequential UPDATE program library with a listing and description of the contents stored with deckname DIRECTORY in the program library and listed in Table 6.

3. CALCULATED RESULTS

3.1 Base Case Category

The base case category calculations, Runs A-1 and A-2, were performed to establish a reference calculation for the sensitivity studies. Due to an error in initial deck preparation, the ECC injection point for Run A-1 was into the inlet annulus and not into the cold legs as desired. Injection into the inlet annulus will result in a smaller primary system depressurization following accumulator injection than would occur if injection was into the cold legs. Reference 2 discusses the effect of alternate ECC injection locations (including the downcomer inlet annulus) on the results of a 0.1016 m cold leg break calculation for the Zion I reactor.

The calculated pressure response of the primary system is shown in Figure 7 for both calculations. Following break initiation for Run A-1, primary pressure decayed rapidly until the hot leg saturated at 7200 kPa (t = 40 s), repressurized slightly for approximately 70 s, and then depressurized until stabilized at 6600 kPa by the steam generator secondaries (t = 140 s). The primary system pressure for Run A-1 remained at approximately the secondary side pressure shown in Figure 8 and 410 s. After 410 s, the secondary side of the steam generators refilled between 140 s to 13.4 m, reducing the auxiliary feedwater flow. The primary system depressurized down to the accumulator setpoint of 4140 kPa at 660 s after the break for Run A-1.

The primary system pressure calculated for Run A-2 depressurized rapidly to 8480 kPa by 120 s where the pressure reached and was stabilized by the steam generator secondary side temperature. As shown in Figure 8, the secondary side pressure calculated for Run A-2 exceeded the safety valve setpoint pressure causing the valves to open at approximately 25 seconds. Auxiliary feedwater flow decreased the secondary side pressure during Run A-2 below the safety valve setpoint by 370 s. Primary and

secondary side system pressures depressurized at the same rate until 510 s in Run A-2. Beyond 510 s, the primary system depressurized faster than the secondaries in Run A-2 due to increased fluid enthalpy of the break flow following break uncovery with accumulator initiation occurring at 995 s.

The mixture level of the upper plenum, upper core volume and middle core volume are shown in Figure 9. The upper plenum and upper core mixture levels indicate upper plenum voiding in both Run A-1 and A-2. For Run A-1, the mixture level remained in the upper plenum with no core uncovery calculated. In Run A-2, core uncovery was calculated to begin at 730 s and continue until the mixture level was 2.0 m below the top of the core at 940 s. The mixture level remained at this elevation until injected accumulator water refilled the core at 1030 s. As seen in Figure 10, no core heatup was calculated during Run A-1, whereas, Run A-2 calculated a heatup of the fuel rod surface in the top 2.0 m of the core reaching a maximum surface temperature of 875 K at 990 s.

Based on these results, Run A-2 was chosen as the reference calculation for the sensitivity study. The choice was based primarily on the prediction of partial core uncovery and a resultant fuel rod cladding heatup. A model resulting in a core heatup was required for the heat transfer sensitivity studies documented in Reference 4.

3.2 Downcomer Noding Category

The downcomer noding category calculations were performed to determine the sensitivity of the calculated results to downcomer nodalization for a small break LOCA. Runs B-1 and B-2 were run to determine if a single volume representation of the downcomer and inlet annulus would improve the computer running time for small break LOCA's without significantly affecting the results. Runs B-3 and B-4 were performed to determine the effect on the reference calculation of using a finer input nodalization for the inlet annulus and downcomer regions.

The changes in the input model between the base cases (Runs A-1 and A-2) and the single volume downcomer-inlet annulus model (Runs B-1 and B-2) necessitated combining two volumes with disimilar geometries. The downcomer inlet annulus was modeled for Runs A-1 and A-2 with a flow area of 18.6 m^2 rather than the geometrical flow area of 2.89 m^2. A large value for the flow area was inherited from the BE/EM study[5] which used a large flow are to produce a pressure in the inlet annulus near the stagnation pressure. The single volume representation of the downcomer and inlet annulus used a flow area equal to the geometrical downcomer flow area of 2.45 m^2 yielding a RELAP4 calculated equivalent flow length of 9.16 m as compared with 5.55 m in the two volume representation. To obtain the same frictional pressure drop between the downcomer nodalization schemes, the equivalent diameter was increased from 0.25 m for the the downcomer in the two volume representation to 0.41 m for the single volume representation. This procedure of volume combination preserved volume, frictional pressure drop, and volume height.

The calculated downcomer and downcomer inlet annulus mixture levels for Runs A-1 and B-1, shown in Figure 11, remained in the downcomer annulus during the entire transient. The calculated levels for both calculations were essentially identical until accumulator initiation was calculated in Run A-1 at 660 s and the downcomer inlet annulus refilled. Due to the slight differences in calculated primary system depressurization rates (Figure 12), Run B-1 did not calculate accumulator initiation with subsequent downcomer refill until 730 s. Following initiation of accumulator injection a slight increase in system pressure was calculated for Run A-1 which terminated accumulator flow (Figure 13) until the primary system pressure again decreased below the accumulator pressure at 1020 s. Run B-1 did not calculate an increase in primary system pressure following accumulator initiation due to accumulator injection into a combined downcomer and inlet annulus volume whereas for Run A-1 the accumulator was injecting only into the downcomer annulus only. Reference 2 discussed calculations performed to determine the effect of alternate ECC injection locations on the calculated primary system pressure during a 0.1016 m cold leg break transient in Zion I. As occurred with Run A-1, Run B-1 did not calculate a significant heatup of the core.

The effect of a single volume nodalization of the downcomer and inlet annulus region (Run B-2) on the results of the reference calculation (Run A-2) were similar to those obtained between Runs A-1 and B-1. The calculated primary system pressure, shown in Figure 14, indicates that a single volume model (Run B-2) produced in a slightly slower depressurization of the primary system after about 800 s. As a result, accumulator initiation during Run B-2 was calculated to occur at 1095 s, which was 100 s later than in the reference calculation (Run A-2). The mixture level in the downcomer and inlet annulus region are shown in Figure 15. As indicated in Figure 15, the mixture level was calculated to decrease into the downcomer in both calculations. The calculated mixture level response was essentially identical for both calculations prior to 903 s at which time Run A-2 calculated the downcomer to refill. A steady drop in the downcomer mixture level between 600 s and 1025 s was calculated for Run B-2. The mixture level remained between 3.8 and 4 m above the bottom of the downcomer until 1095 s when accumulator initiation refilled the downcomer to the top of the inlet annulus.

The increase in downcomer mixture level at 903 s calculated for Run A-2 was a direct result of using the RELAP4/MOD7 mixture level crossing model[1] during a restart. The mixture level crossing model is a new iterative solution technique that was developed to improve the predictions of junction flow rates in RELAP4/MOD7. Prior to 903 s, the calculation used an average time step size of 0.1 ms requiring 1460 CYBER 176 cpu seconds/transient second. The relatively small time step was a result of code calculated mass depletions (more liquid calculated leaving a volume than was available) in the upper head and inlet annulus. Activation of the mixture level crossing model at 903 s increased the running efficiency to 159 cpu seconds/transient second with an increase in the average time step size to 0.67 ms. Based on the improvement in running time, the decision was made to use the mixture level crossing model for all future calculations in the sensitivity study (Runs B-3, B-4, and all category C, D, and E calculations) with the model activated at problem initiation.

Analysis performed after completion of the calculations indicated that the model may not be working correctly. As seen in Figure 15, implementaton of the mixture level crossing model in Run A-2 at 903 s forced the downcomer mixture level to return to the junction between the downcomer and the inlet annulus instead of allowing it to continue dropping into the downcomer as calculated for Run B-2. The junction between the inlet annulus and the downcomer does not constitute a geometric boundary in the system being modeled and should be passive to mixture levels crossing through. An explanation for the anomolous results obtained with the mixture level crossing model is not known at this time. The mixture level crossing model and its interaction with other code models (stacked volume level tracking, slip, bubble rise) needs to be investigated further to determine the cause of the mixture level tracking calculational difficulties when the mixture level crossing model is used.

The calculated upper plenum, upper core volume and middle core volume mixture levels, shown in Figure 16, were essentially identical for both Runs A-2 and B-2 until 400 s. After 400 s, the results for Run A-2 show the mixture level dropped to the top of the core at 670 s and to an elevation 2 m below the top of the core by 925 s. The level remained 2 m below the top of the core until accumulator flow forced the mixture level back into the upper plenum by 1040 s. The sudden drop in mixture level at 903 s was the result of restarting the calculation with the mixture level crossing model activated. Run B-2 calculated a drop in the mixture level of 1.3 m below the top of the core. Initial accumulator flow induced steam condensation in the cold legs, downcomer, and inlet annulus reduced the core level to an elevation which was 2.6 m below the top of the core by 1020 s. This decrease in the core level was followed immediately by a refill of the core caused by injected accumulator liquid. As seen in Figure 17, the calculated peak cladding temperature was higher in Run A-2 than in Run B-2 due to the longer period of core uncovery calculated in Run A-2.

Using a more detailed nodalization to model the downcomer and inlet annulus region was evaluated with Runs B-3 and B-4. Run B-3 utilized the same model used for the reference calculation (Run A-2), however, the inlet annulus was split into two vertically stacked volumes. The annulus was arbitrarily split at an elevation of 1.27 m above the cold leg centerline. This elevation was equal to the distance between the cold leg centerline and the top of the downcomer volume. Run B-4 used the reference calculation model, with the single downcomer volume replaced with the three volume downcomer representation used in Reference 5.

The calculated primary system depressurization rate for Runs A-2, B-3, and B-4 were essentially identical, as shown in Figure 18. A significant difference between the three calculations was in the downcomer and inlet annulus mixture level response shown in Figure 19. As previously stated, the RELAP4/MOD7 mixture level crossing model was activated at problem initiation in both Runs B-3 and B-4. As the mixture level decreases below the upper inlet annulus volume in Run B-3 at 295 s, code calculated mass depletions were calculated to occur in that volume causing the two observed spikes in the mixture level between 300 and 350 s. The spikes result from the code attempting to return the mixture level to the junction between the two inlet annulus volumes. The mixture level calculated in Run B-3 dropped initially then increased to an elevation corresponding to the bottom of the cold leg junction by 720 s. The mixture level dropped to the top of the downcomer by 850 s where it remained until accumulator injection refilled the inlet annulus at 1010 s. The mixture level calculated in Run B-4 was identical to that calculated by the reference calculation (Run A-2) until it reached to top of the downcomer at 770 s. Calculated mass depletions in the inlet annulus in Run B-4 after 770 s resulted in the mixture level remaining at the junction between the downcomer and inlet annulus until accumulator injection refilled the inlet annulus at 1030 s.

The calculated upper plenum upper core volume, and middle core volume mixture level for Run B-3, are shown in Figure 20. As indicated on Figure 20, the mixture level remained above the top of the core until 870 s. The mixture level then dropped 1.3 m into the core where it

remained until accumulator flow refilled the core. Run B-4 calculated essentially the same level response as the reference calculation with some minor differences in calculated response observed between 800 s and 1000 s.

A peak cladding surface temperature of 750 K was calculated for Run B-3 and as shown in Figure 21, was 125 K lower the temperature calculated for the reference calculation (Run A-2). There was no significant differences between calculated cladding surface temperatures for Runs B-4 and A-2.

The computer running time for the downcomer noding study are given in Table 7. Although the reference calculation, Run A-2, appeared to have run slower than Run B-2 or B-4, most of the difference is related to not using the mixture level smoothing model prior to 903 s. It is estimated that the computer time required with the mixture level crossing model active for the entire tranient would be 4.5 to 5.0 hours. The comparatively large running time required for Run B-3 was due almost entirely to the excessive number of mass depletions calculated for the upper inlet annulus volume and the lower inlet annulus volume.

The results of the downcomer noding study were not conclusive enough to recommend any particular nodalization scheme since the RELAP4/MOD7 mixture level crossing model appeared to have had a major effect on the results. Further study is needed to determine if an error exists in the mixture model. An iterative solution technique for junction flows such as the mixture level crossing model is required to reduce computer time requirements.

3.3 Cold Leg Modeling Study

The cold leg modeling study was performed to investigate the effect of modeling phase separation in the cold legs on the results of the reference calculation. The calculation was also used as part of the circumferential break location study, discussed in Section 3.4.

The changes made to the reference model (Run A-2) for Run C were inclusion of the Wilson bubble rise model in all volumes between the pump outlets and the vessel and modeling of the break junction as a vertically oriented junction with the junction centered at the cold leg midplane.

The calculated cold leg mixture level at the break, shown in Figure 22, dropped from the top of the cold leg at 230 s to the top of the break junction at 250 s. The mixture level dropped through the break junction between 250 and 600 s and remained near the bottom of the junction until accumulator injection refilled the volume at 965 s. A comparison of calculated break mass flow for the reference calculation (Run A-2) and Run C, shown in Figure 23, shows essentially identical results. The calculated break flow for Run C did exhibit unstable behavior when the mixture level in the cold leg was near the bottom of the break junction.

The calculated behavior of the downcomer and downcomer inlet annulus mixture level for Run C, shown in Figure 24, was similar to that observed for the downcomer noding calculation. With the mixture level crossing option activated, the mixture level dropped to the top of the downcomer at 700 s and remained there until accumulator injection refilled the vessel at 980 s. The behavior is not believed to be realistic after 700 s since the level should continue to drop into the downcomer.

The inclusion of phase separation in the cold legs resulted in an increase in the computer time requirements, as seen in Table 7. The additional time requirements are related to applying the Wilson bubble rise model to the cold legs.

The use of phase separation in the cold legs should also be coupled with a horizontal phase slip model in connecting junctions. If the phases are not allowed to flow independently between the cold leg volumes, the calculated volume average fluid energy is used for the connecting fluid energy. The calculation would then be equivalent to using homogeneous assumptions in the cold leg. RELAP4/MOD7 does not contain a recommended

model for horizontal slip and therefore one was not used. The lack of a horizontal slip model coupled with the increased computer running time suggests that phase separation modeling in the cold legs is not viable at this time. However, the effect of the mixture level crossing model on the results excludes any diffinative conclusion. The recommendation is to resolve the difficulties with the mixture level smoothing model and develop a horizontal slip model before pursuing phase separation modeling in the cold legs.

3.4 Break Circumferential Location Study

The break circumferential location study was performed to determine if the results of the Run C calculation with phase separation in the cold legs were dependent upon the circumferential location of the break. The locations investigated were the top of the cold leg pipe (Run D-1), the bottom of the cold leg pipe (Run D-2), and 0.015 m above the bottom of the cold leg pipe (Run D-3).

The changes made in the Run C calculation model was the break junction treated as a horizontally oriented (point) junction for all the Run D series calculations.

Calculational instabilities in the Run D-2 calculation forced termination of the calculation at 428 s. The break at the bottom of the pipe drained all of the liquid out of the cold leg by 300 s resulting in unresolvable mass depletion problems in the cold leg. As a resolution to the problem, Run D-3 was performed with the break located 0.015 m above the bottom of the cold leg pipe to allow a small amount of liquid to remain in the pipe.

The results of the calculations showed that the break location did not have a significant effect on the results of the Run C calculation. The broken loop cold leg mixture levels, shown in Figure 25, were calculated to drop to the respective break junction elevations by 300 s (top of the

junction for Run C). The levels remained at these elevations until accumulator initiation refilled the cold legs at 980-990 s. The integrated mass flow out the break shown in Figure 26 and calculated upper plenum pressure shown in Figure 27 indicate virtually identical results for all three calculations.

The computer cpu time requirements, shown in Table 7, were of the same order of magnitude for all of the calculations with cold leg phase separation. For comparison with the Run D-2 calculation, Run C required 1.5 hours to calculate the first 430 s of the transient.

The results of the study indicate that break location was not an important consideration for a small break calculation with phase separation in the cold legs. However, the considerations and recommendations detailed in the cold leg modeling study discussed in Section 3.3 also apply to the circumferential break location study.

3.5 Nonequilibrium Modeling Study

The nonequilibrium modeling study was performed to examine the effect of the RELAP4/MOD7 nonequilibrium model on post accumulator injection system response. The model was activated just prior to accumulator initiation at 930 s. This study was performed by restarting from Run A-2 which modeled homogeneous cold leg and from Run C which modeled phase separation in the cold legs.

The nonequilibrium model did not require any changes in modeling. The model was applied to all cold leg and vessel volumes with the recommended or code default values used for input in Run B-1 (homogeneous) and Run E-2 (phase separation). The recommended or default input were: (a) the model remained on regardless of the volume quality, (b) the flow-regime dependent contitutive package was used, (c) the multiplier for the interfacial heat transfer rate was 1.0, and (d) the weighting factor constant used for calculating interphase heat transfer rate in the transition regions was

1.0. A third calculation, Run E-3, was performed with the multiplier for the interfacial heat transfer rate set to 0.5 to determine the sensitivity of the results of Run E-2 to this parameter.

The calculated primary system pressure response for Runs A-2 and E-1 are shown in Figure 28 after 900 s. The nonequilibrium calculation, Run E-1, shows a more gradual post-accumulator injection primary system pressure response than that obtained with the equilibrium calculation in Run A-2. The slower depressurization after accumulator initiation for Run E-1 altered the accumulator flow response. The accumulator flow, shown in Figure 29 was much less for Run E-1 than that calculated in Run A-2. As a result, the core refilled slower in Run E-1 than Run A-2 as shown in Figure 30. The calculated cladding surface temperature at the top of the core for Run E-1 showed a much slower cooldown after accumulator initiation than did Run A-2 as shown in Figure 31.

A decrease in the core mixture level, shown in Figure 30, was calculated at 930 s, the time at which the nonequilibrium model was tripped on. Since no other changes in the transient occur at this time, the level drop was solely related to the nonequilibrium model activation. Further study is required to determine how the nonequilibrium model interacts with the Wilson bubble rise and vertical slip models in RELAP4/MOD7 to produce this effect on mixture levels.

The primary system pressure response for the calculations with phase separation modeled in the cold legs (Runs C, E-2, and E-3) are shown in Figure 32 and the results exhibited the same trends as the calculations performed with homogeneous cold leg volumes. The dip in the primary system pressure for Run E-3 at 980 s occurred when the broken loop cold leg became water solid. The broken loop cold leg mixture level shown in Figure 33 was calculated to start decreasing when the nonequilibrium model was activated at 930 s for Runs E-2 and E-3. The rate and magnitude of the drop in level were dependent on the condensation rate. Run E-3 modeled a condensation rate 0.5 times the value used for Run E-2. Run E-2 calculated the cold leg

mixture level returning to the bottom of the break at accumulator initiation, where the mixture level remained for the rest of the transient. Run E-3 calculated the cold leg liquid full after accumulator initiation despite a lower interphase heat transfer rate than was modeled in Run E-2. The exact reasons for this behavior have not yet been identified and will require further study to understand.

The integrated mass flow out of the broken loop accumulator, shown in Figure 34, was much lower for Runs E-2 and E-3 due to the higher primary system backpressure As a result, the calculated core mixture level for Runs E-2 and E-3 rose much slower than the core mixture level calculated by Run C, as shown in Figure 35. The corresponding peak rod surface temperatures in the top third of the core, shown in Figure 36, was higher for the calculations with nonequilibrium. A calculated peak cladding temperature of 1050 K for Run E-2 was 175 K higher than the 875 K peak temperature calculated in the Run A-2 reference calculation.

The computer run time for Run E-1 nonequilibrium model calculation was of the same magnitude as the equilibrium case Run A-2 (see Table 7). However, for the case with phase separation in the cold legs, the computer time requirements between 930 and 1189 s for the Run E-2 and E-3 nonequilibrium calculations were more than triple that of the homogeneous calculation Run C.

The results show a marked improvement in the post-accumulator injection transient response. The system pressure calculation and accumulator flow rates were typical of expected results when the nonequilibrium model was used. However, interactions between the nonequilibrium model and the phase separation models in RELAP4/MOD7 need to be investigated further. Further assessment of the nonequilibrium model is also required to evaluate the user supplied input parameters to the nonequilibrium model.

4. CONCLUSIONS AND RECOMMENDATIONS

1. *Use of the RELAP4/MOD7 mixture level crossing model resulted in the downcomer mixture level not being calculated correctly.*

The mixture level crossing model forced the mixture level to remain in the proximity of volumes in which liquid mass depletions were calculated by RELAP4/MOD7. The atypical mixture level behavior was particularly evident in the downcomer and inlet annulus regions. Sensitivity of the results of the reference calculation to downcomer noding (Section 3.2) were indiscernible due to mixture level calculational aytpicalities associated with the mixture level crossing model. Calculations in which the mixture level crossing model was not used or the junction between the inlet annulus and the downcomer was not modeled predicted the mixture level dropping into the downcomer volume. Use of the mixture level crossing model forced the level to remain at the junction separating the inlet annulus and the downcomer.

2. *Phase separation modeling in the cold legs is not recommended until an accurate horizontal slip model is developed.*

Modeling of phase separation in the cold legs without horizontal slip in connecting junctions is equivalent to using horizontal assumptions in the cold legs (Section 3.3). The circumferential location of the break is unimportant unless phase separation is modeled in the cold legs (Section 3.4).

3. *The RELAP4/MOD7 nonequilibrium model requires further assessment before guidelines for its use can be recommended.*

Use of the RELAP4/MOD7 nonequilibrium model (Section 3.5) results in more typical system pressure response when accumulator water is injected into steam filled volumes. Interactions betwen the nonequilibrium model, bubble rise model, and mixture level crossing model need to be investigated further before recommendations for use can be made.

REFERENCES

1. RELAP4/MOD7, Users Manual, EG&G Idaho, Inc., (To be published).

2. C. D. Fletcher, Additional Audit Calculations for Westinghouse PWR Small Breaks, EG&G Idaho, Inc., EGG-CAAP-5052, November 1979.

3. C. D. Fletcher et al., Loss of Offsite Power Scenarios for the Westinghouse Zion I Pressurized Water Reactor, EG&G Idaho, Inc., EGG-CAAP-5156, May 1980.

4. J. C. Lin, RELAP4/MOD7 Nodalization and Heat Transfer Sensitivity Calculations for Zion Plant During Small Break LOCA, EGG-CAAP-5320, December 1980.

5. G. W. Johnsen et al., A Comparison of "Best Estimate" and "Evaluation Model" LOCA Calculations: The BE/EM Study, EG&G Idaho, Inc., PG-R-76-009, December 1976.

APPENDIX A

METRIC TO ENGLISH CONVERSION FACTORS

The following list of conversion factors are supplied for converting data presented in the text of the report from metric to English.

To Convert From	to	Multiply by
Pa	lb_f/in^2	1.450×10^{-4}
Kg/sec	lbm/sec	2.205
K	°F	$T_{°F} = 1.8 \times T_k - 459.67$
m	ft	3.281
ℓ/s	gpm	15.850
rad/s	rpm	9.55

TABLE 1. SENSITIVITY CALCULATION MATRIX

Category	Run Index	Calculational Description
Base case	A-1	Best-estimate initial and boundary conditions.
	A-2	Evaluation model initial and boundary conditions.
Downcomer Noding	B-1	Run A-i with single volums representation of downcomer and downcomer inlet annulus.
	B-2	Run A-2 with single volume representation of downcomer and downcomer inlet annulus.
	B-3	Run A-2 with two volume representation of downcomer inlet annulus.
	B-4	Run A-2 with three volume representation of downcomer.
Phase separation in cold legs	C	Run A-2 with phase separation modeled in cold leg volumes. (Break location at pipe mid-plane).
Break Circumferential Location	D-1	Run C with the break located at the top of the cold leg pipe
	D-2	Run C with the break located at the bottom of the cold leg pipe.
	D-3	Run C with the break located .015 m above the bottom of the cold leg pipe.
Nonequilibrium Model	E-1	Run A-2 with the RELAP4/MOD7 nonequilibrium model tripped on at 930. s with code default/ recommended input values.
	E-2	Run C with the RELAP4/MOD7 nonequilibrium model tripped on at 930 s with code default/ recommended input values.
	E-3	Run E-2 with interfacial heat transfer rate multiplier (DECCMX) reduced from 1.0 to 0.5.

TABLE 2. SAFETY INJECTION FLOW RATE AS A FUNCTION OF PRIMARY SYSTEM PRESSURE--BEST ESTIMATE

Primary Pressure (MPa)	Injection Rate Per Loop (ℓ/s)
0.1034	73.49
0.2413	62.33
0.3792	51.48
0.5171	40.31
0.7239	28.07
0.8824	15.58
1.482	15.01
4.709	14.07
5.784	12.55
7.466	10.03
8.087	9.021
8.852	7.507
9.776	6.031
9.927	5.021
10.38	3.015
10.54	1.508
11.15	0.0

TABLE 3. CHARGING FLOW RATE AS A FUNCTION OF PRIMARY SYSTEM PRESSURE--BEST ESTIMATE

Primary Pressure (MPa)	Charging Rate Per Loop (ℓ/s)
0.1034	13.31
0.409	13.31
9.314	10.85
11.62	9.642
14.68	7.255
16.22	6.043
18.06	3.627
18.37	0.0

TABLE 4. STEAM GENERATOR SECONDARY DUMP AND SAFETY VALVE FLOW RATE AS A FUNCTION OF SECONDARY SYSTEM PRESSURE--BEST ESTIMATE

Secondary Pressure (MPa)	Mass Flow Rate (Kg/s)
$\leq$7.618	0.0
7.755	545.0
8.238	545.0
8.239	749.9
$\geq$8.618	3086.9

TABLE 5. SAFETY INJECTION RATE AS A FUNCTION OF PRIMARY SYSTEM PRESSURE--EVALUATION MODEL

Primary Pressure Rate (MPa)	Safety Injection Rate Per Loop (ℓ/s)
0.103	77.0
0.241	181.7
0.380	53.9
0.517	42.2
0.724	29.4
0.883	16.3
1.48	15.7
2.86	14.3
4.24	12.8
5.62	11.3
7.00	9.4
8.38	7.5
9.07	6.0
9.96	2.6
11.14	2.0
12.51	1.1
14.31	0
17.24	0

TABLE 6. DESCRIPTION OF INPUT DECKS USED FOR RELAP4/MOD7 SENSITIVITY STUDIES

DECKNAME	RUN INDEX	DESCRIPTION
WBASEDD	A-1	ZION BASE CASE BEST ESTIMATE DECK FOR A 4 INCH COLD LEG BREAK (DERIVED FROM STATION BLACK-OUT DECK).
EMBASE	A-2	ZION BASE CASE EVALUATION MODEL DECK FOR A 4 INCH COLD LEG BREAK (DERIVED FROM ADDITIONAL WESTINGHOUSE AUDIT CALCULATIONS RUN B).
WBASE	B-1	ZION BASE CASE BEST ESTIMATE DECK WITH THE DOWNCOMER INLET ANNULUS AND DOWNCOMER COMBINED INTO A SINGLE VOLUME.
EMONEDC	B-2	ZION EVALUATION MODEL DECK WITH THE DOWNCOMER AND INLET ANNULUS COMBINED INTO ONE VOLUME.
SPANN	B-3	ZION EVALUATION MODEL DECK WITH THE DOWNCOMER INLET ANNULUS SPLIT INTO TWO VOLUMES AXIALLY.
B09DC	B-4	ZION EVALUATION MODEL DECK WITH THE DOWNCOMER REPLACED WITH THE THREE VOLUME DOWNCOMER NODALI-ZATION USED IN THE BE/EM STUDY (TAKEN FROM BEB09).
CBLBASE	C	ZION EVALUATION MODEL DECK WITH PHASE SEPARATION IN ALL COLD LEG VOLUMES WITH THE BREAK JUNCTION LOCATED AT THE PIPE MIDPLANE AND TREATED AS A VERTICALLY ORIENTED JUNCTION.
CBLTOV	D-1	CBLBASE DECK WITH THE JUNCTION ORIENTED AT THE TOP OF THE COLD LEG PIPE AND TREATED AS A HORIZONTALY ORIENTED (POINT) JUNCTION.
CBLBOV	D-2	CBLBASE DECK WITH THE JUNCTION ORIENTED AT THE BOTTOM OF THE COLD LEG PIPE AND TREATED AS A HORIZONTALLY ORIENTED JUNCTION.
CBLABOV	D-3	CBLBASE DECK WITH THE JUNCTION ORIENTED .05 FEET ABOVE THE BOTTOM OF THE COLD LEG PIPE AND TREATED AS A HORIZONTALLY ORIENTED (POINT) JUNCTION.
NONEHO	E-1	RESTART DECK USED WITH EMBASE RESULTS TO TRIP ON THE RELAP4/MOD7 NONEQUILIBRIUM MODEL (DEFAULT AND/OR RECOMMENDED VALUES) AT 930. SEC.
NONEPS	E-2	RESTART DECK FOR CBLBASE RESULTS WITH THE NON-EQUILIBRIUM MODEL TRIPPED ON (DEFAULT AND/OR RECOMMENDED INPUT) AT 930. SEC.

TABLE 7. COMPUTER RUN TIMES FOR THE RELAP4/MOD7 SENSITIVITY STUDIES

Run Index	Transient Time (s)	CDC 176 cp Time (hr)
A-1	0-1027	5.3
A-2	0-1038	6.0
B-1	0.966	4.7
B-2	0-1153	4.9
B-3	0-1045	11.6
B-4	0-1012	4.1
C	0-1250	7.7
D-1	0-1140	7.9
D-2	0-428	3.4
D-3	0-1006	8.1
E-1	930-1159	3.7[a]
E-2	930-1189	6.2[b]
E-3	930-1058	3.4[c]

a. Run E-1 required 1.1 cpu hours from 930 to 1044 s.
Run A-2 required 1.7 cpu hours from 930 to 1038 s.

b. Run C required 1.7 cpu hours from 930 to 1250 s.

c. Run E-2 required 3.1 cpu hours from 930 to 1058 s.

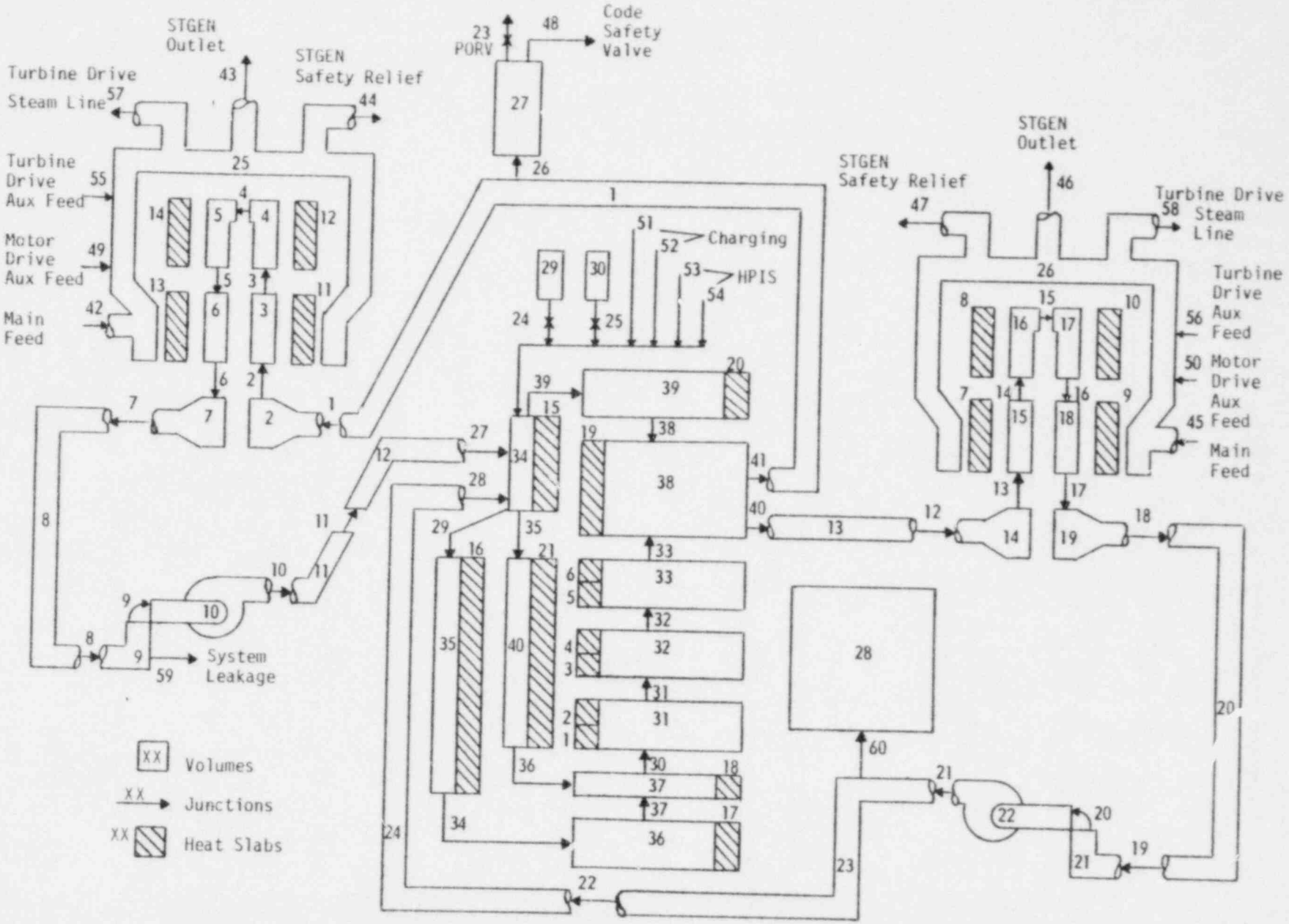

Figure 1. Nodalization for Run A-1.

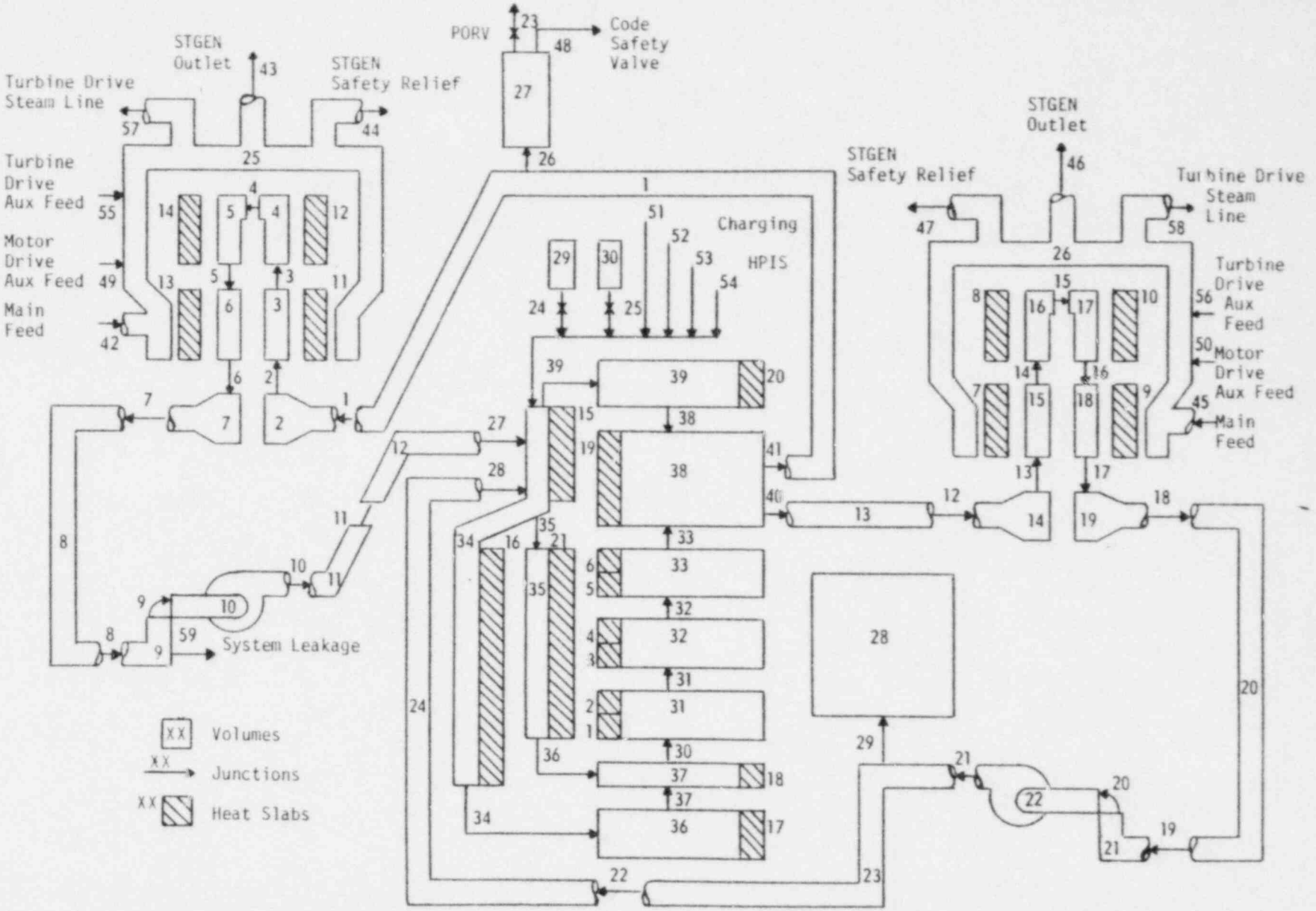

Figure 2. Nodalization for Run B-1.

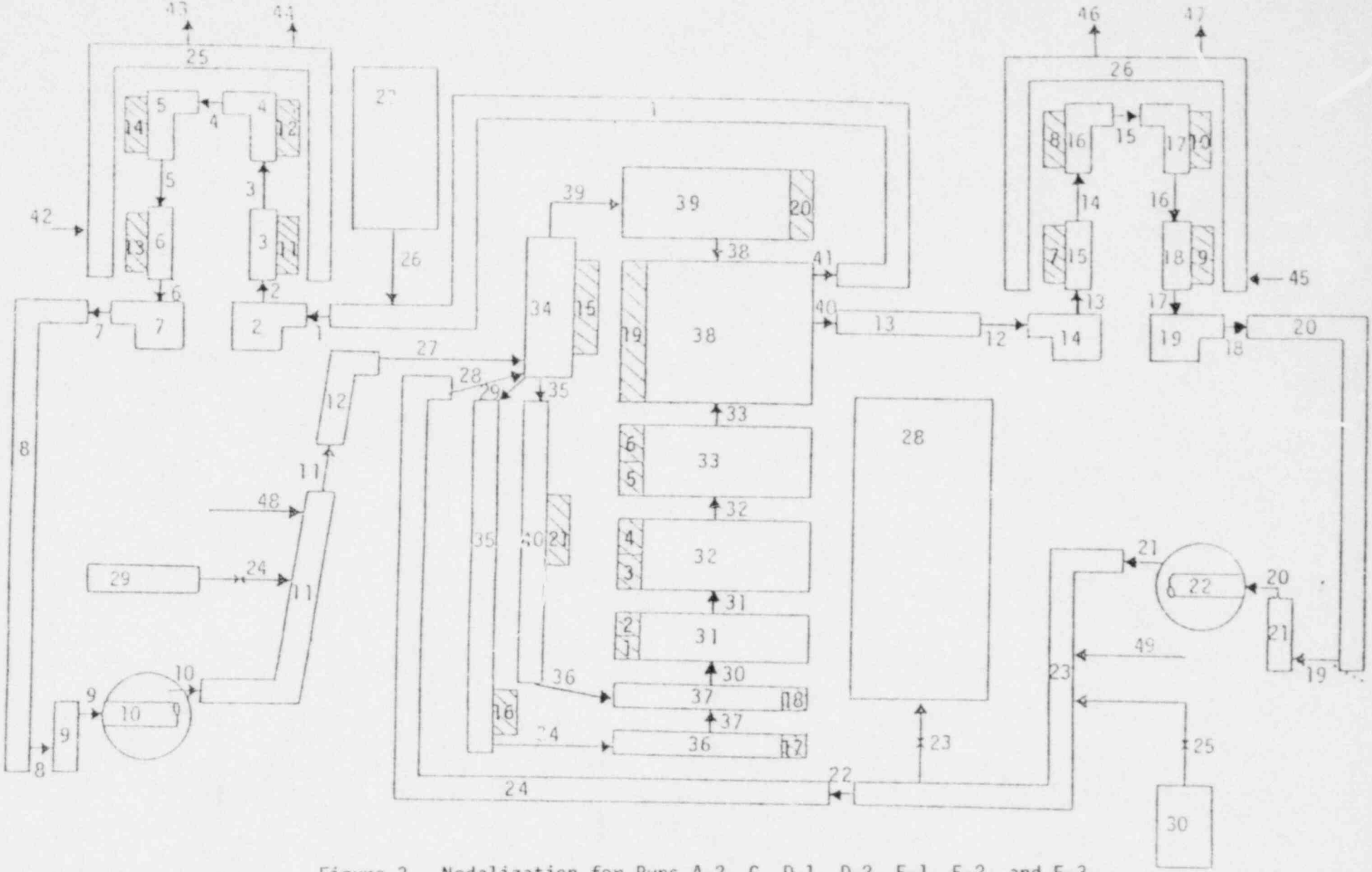

Figure 3. Nodalization for Runs A-2, C, D-1, D-2, E-1, E-2, and E-3.

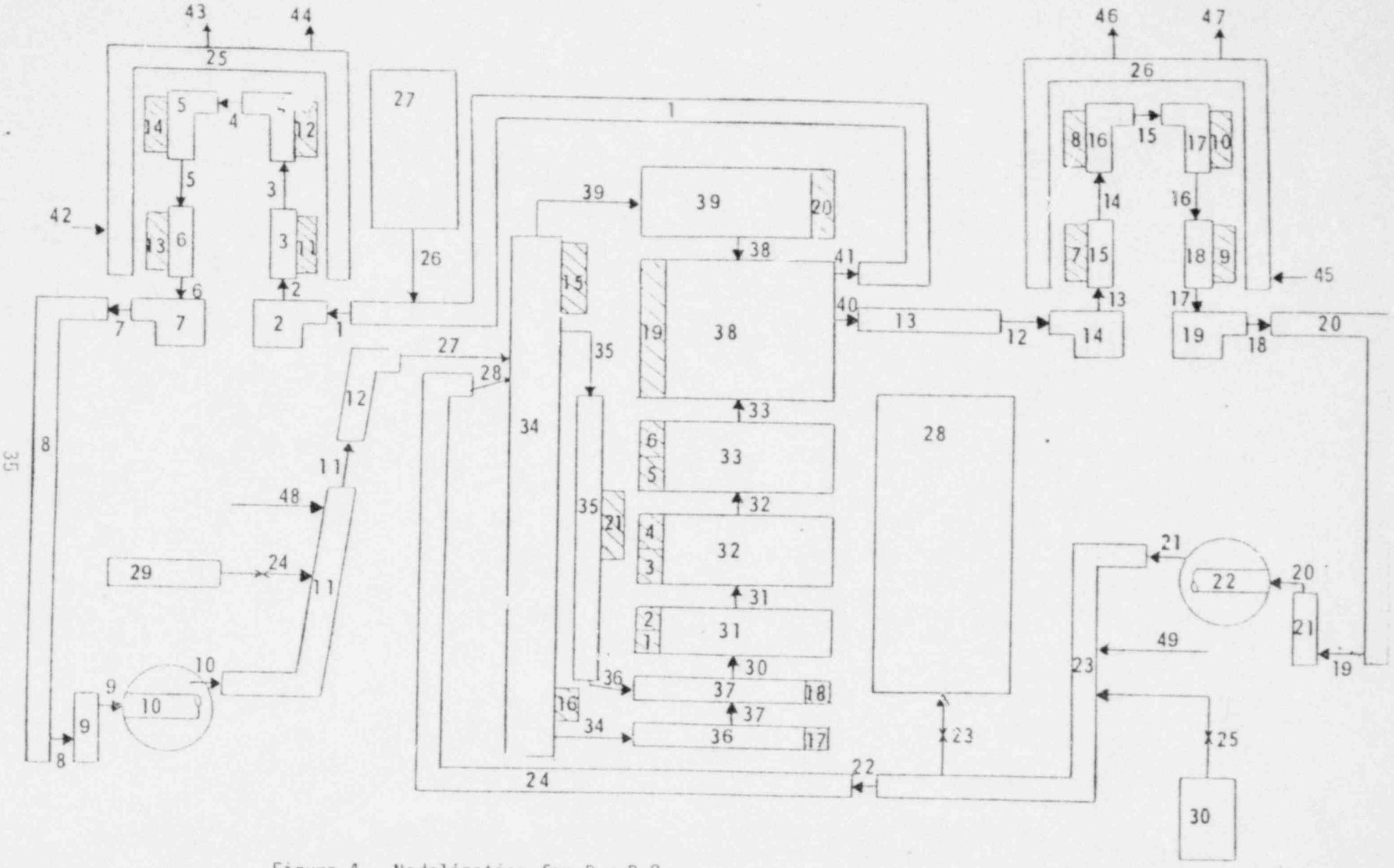

Figure 4. Nodalization for Run 9-2.

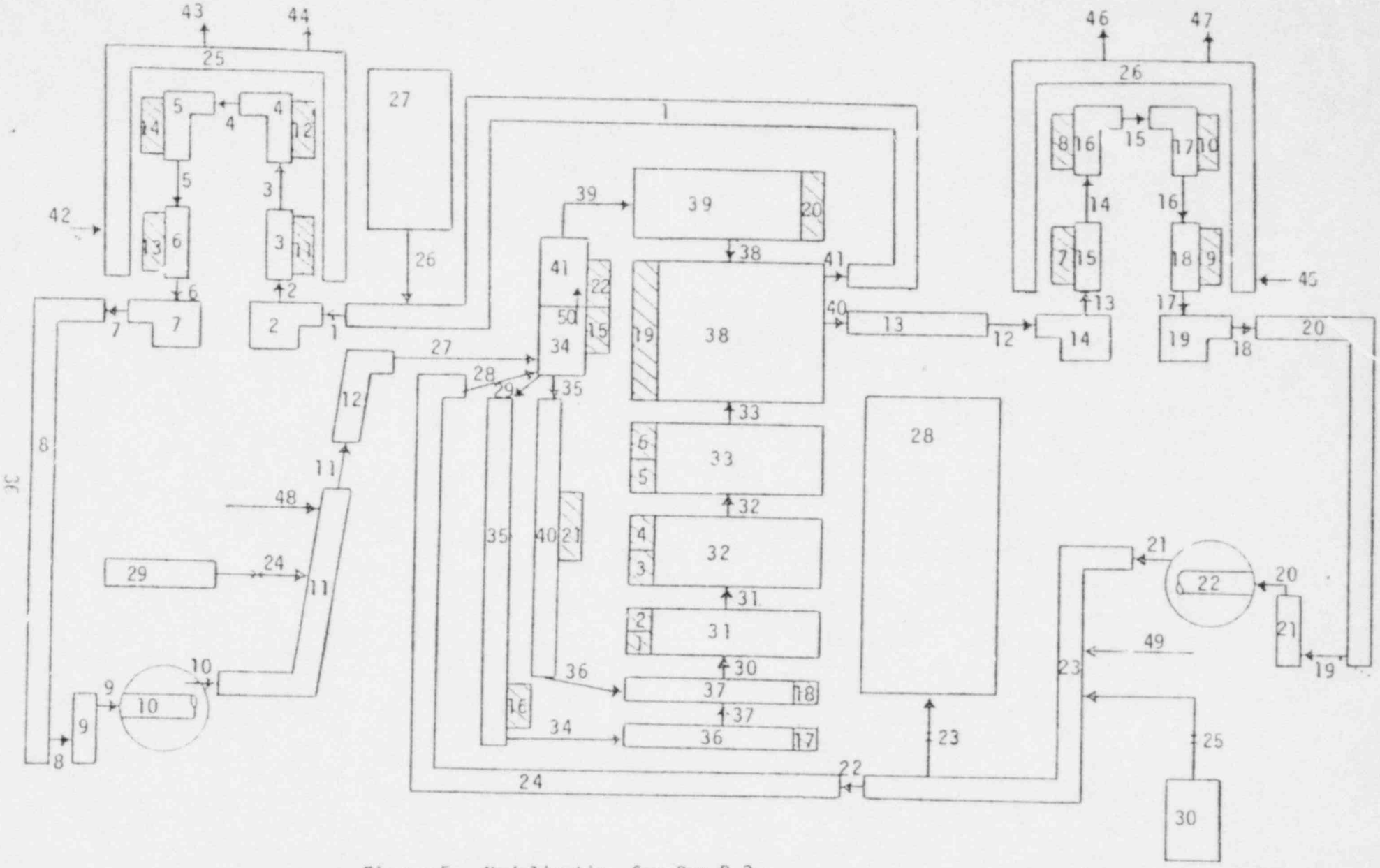

Figure 5. Nodalization for Run B-3.

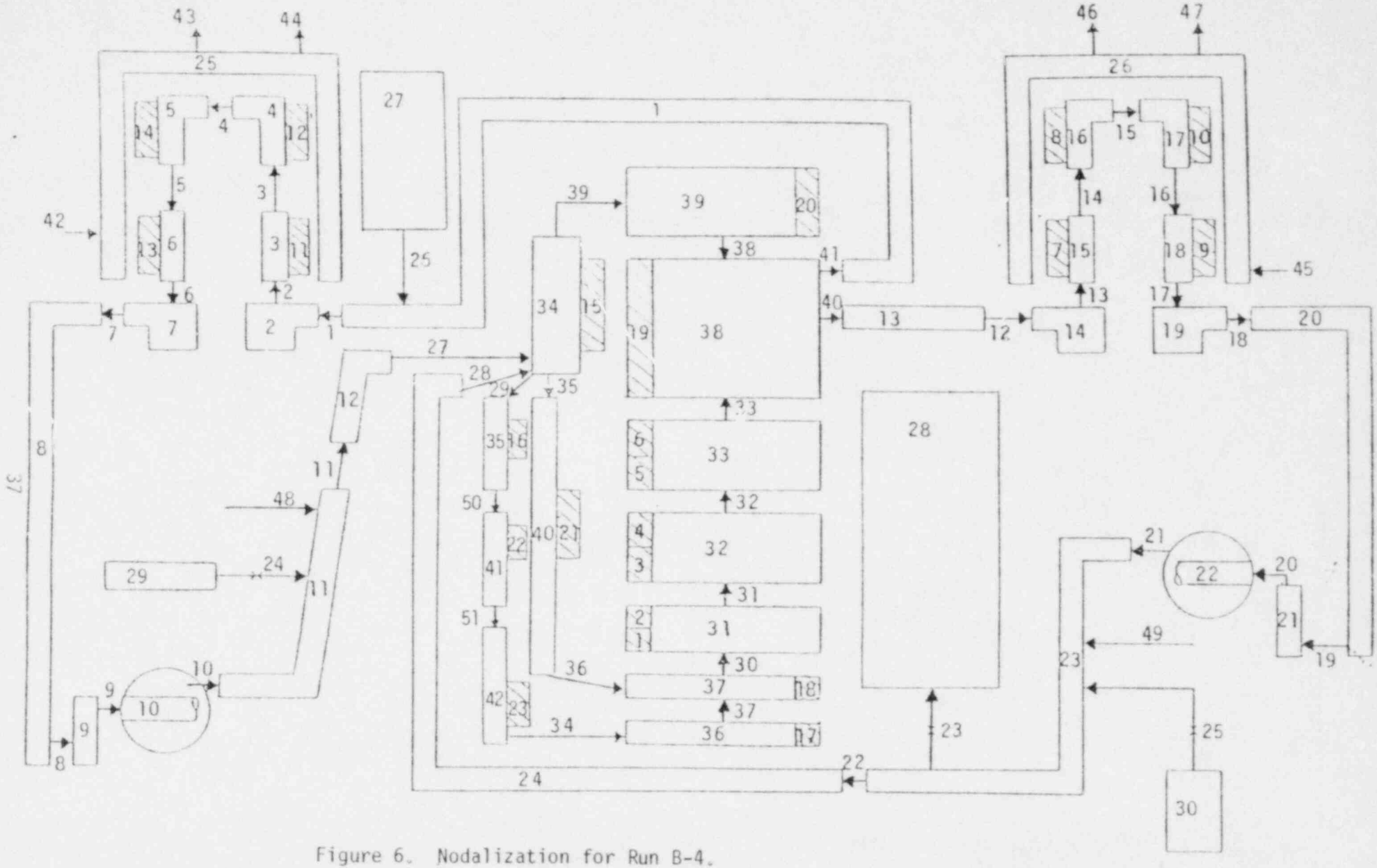

Figure 6. Nodalization for Run B-4.

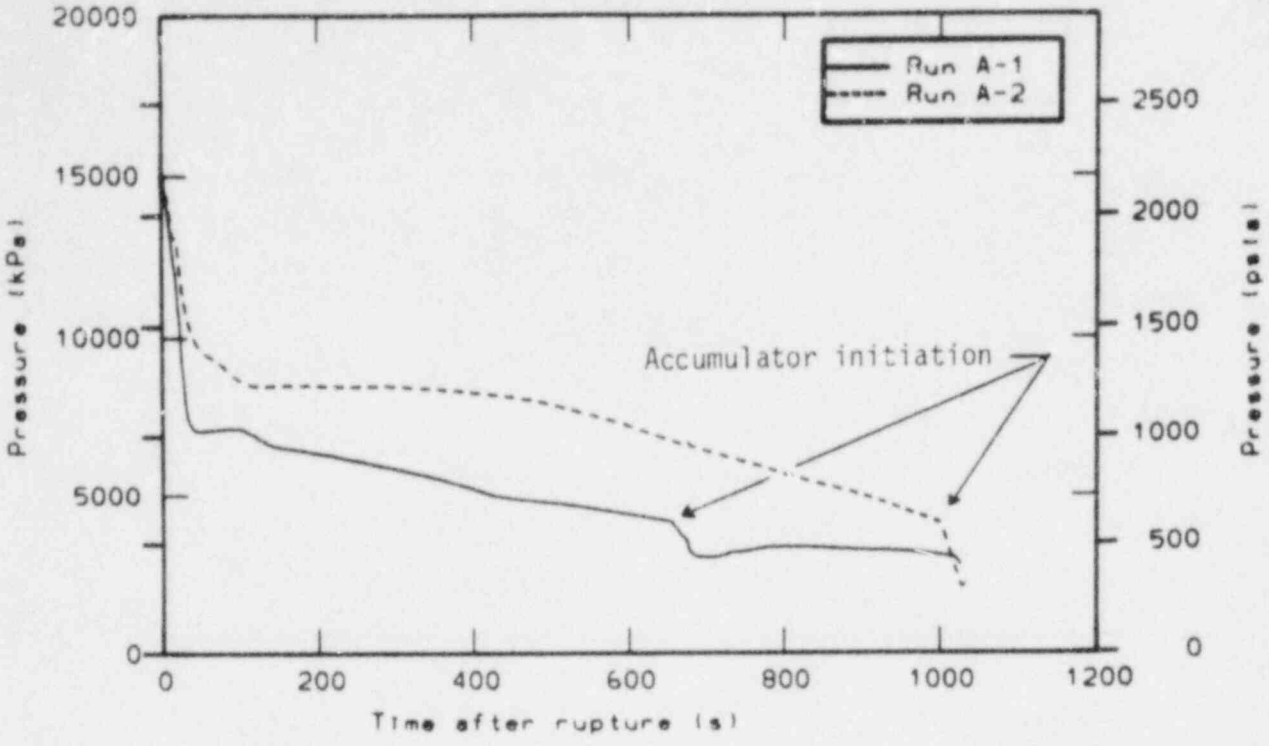

Figure 7. Upper plenum pressure vs. time for Runs A-1 and A-2.

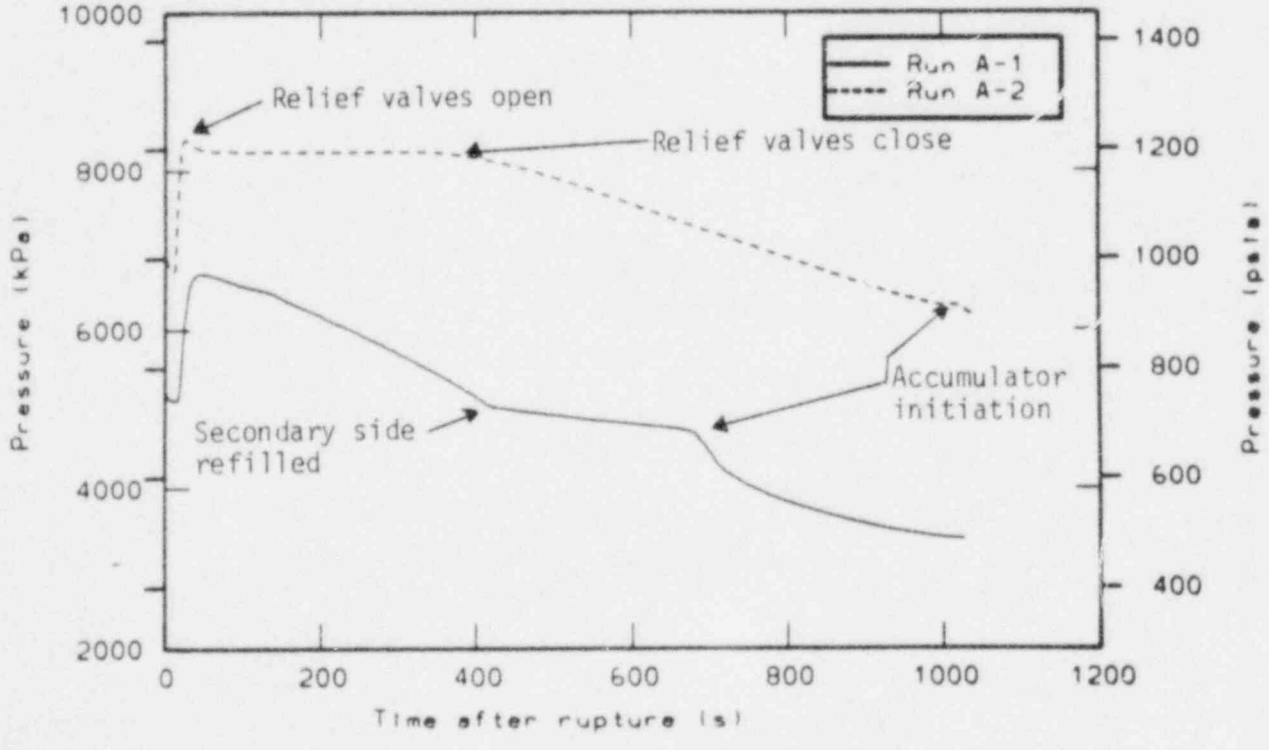

Figure 8. Steam generator secondary side pressure vs. time for Runs A-1 and A-2.

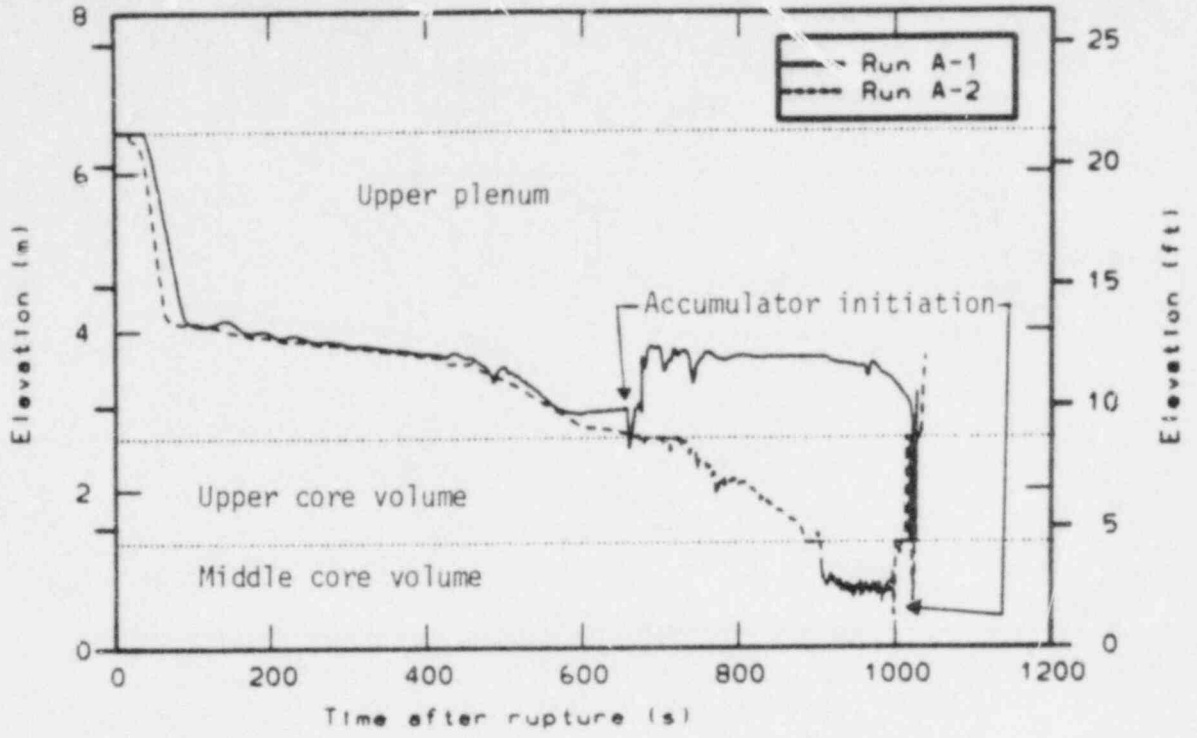

Figure 9. Upper plenum and upper core volume mixture levels vs. time for Runs A-1 and A-2.

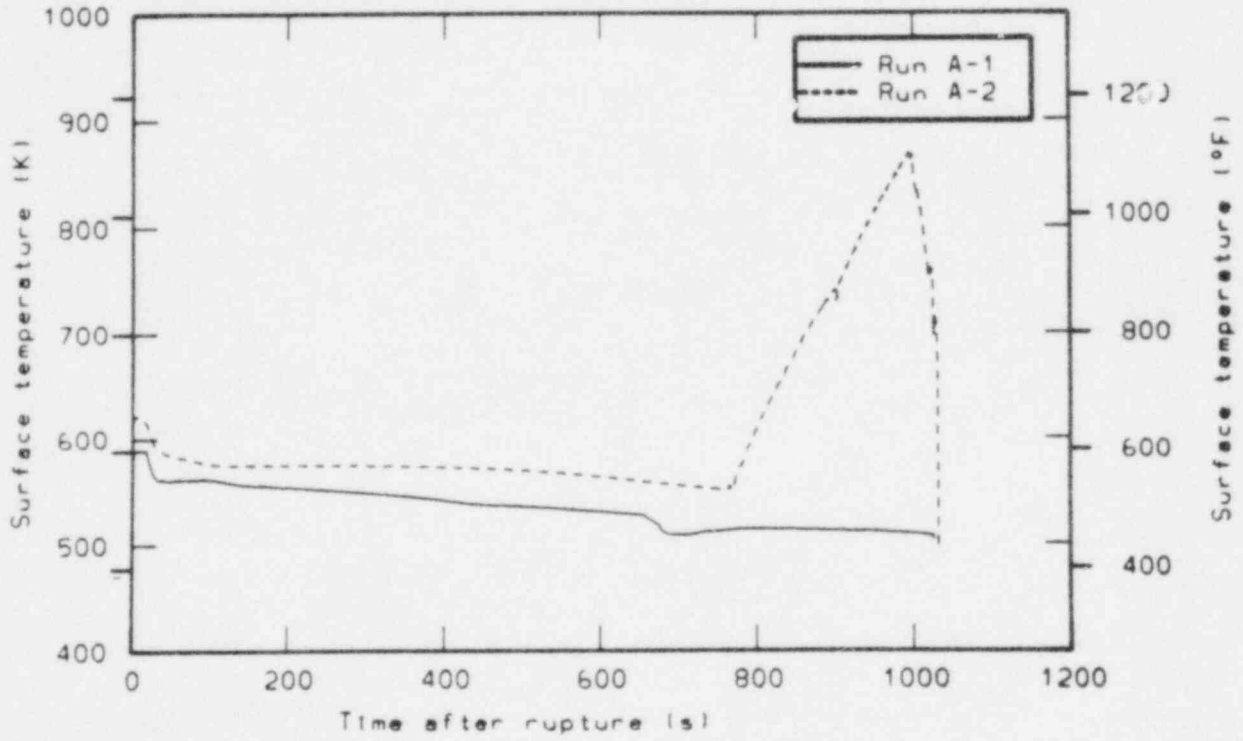

Figure 10. Fuel rod cladding surface temperature 3.0-3.7 m. above the core inlet vs. time for Runs A-1 and A-2.

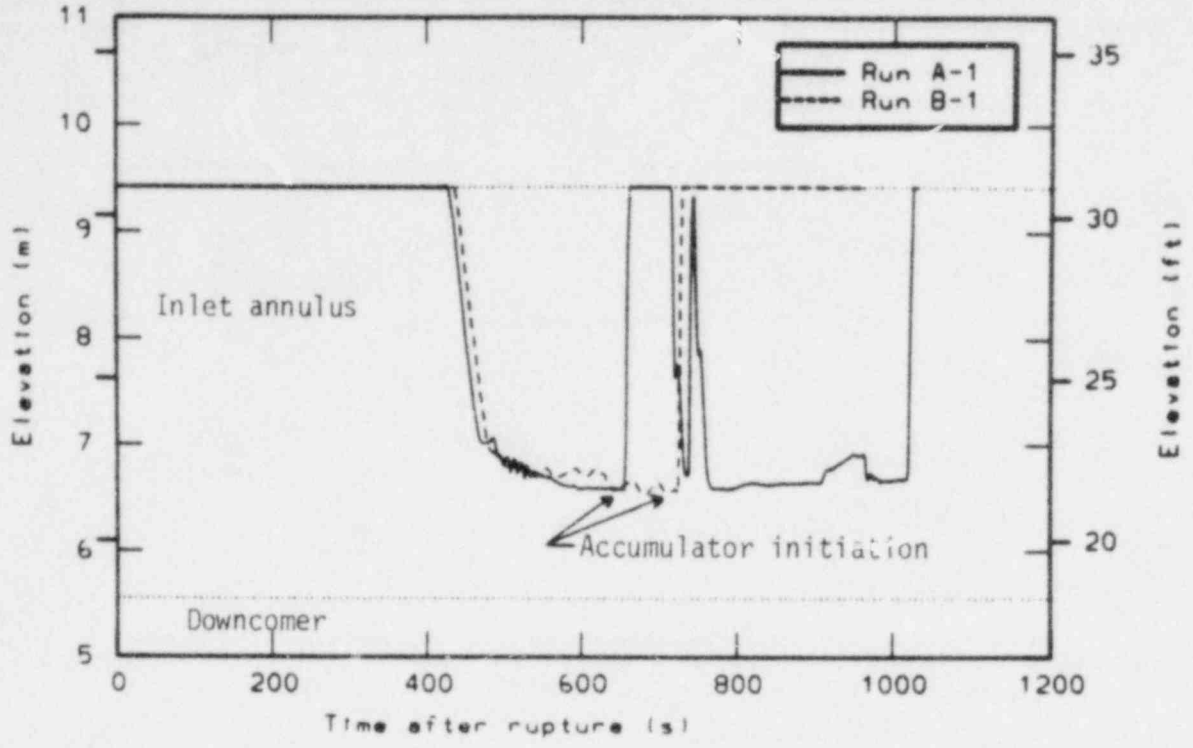

Figure 11. Downcomer and downcomer inlet annulus mixture levels vs. time for Runs A-1 and B-1.

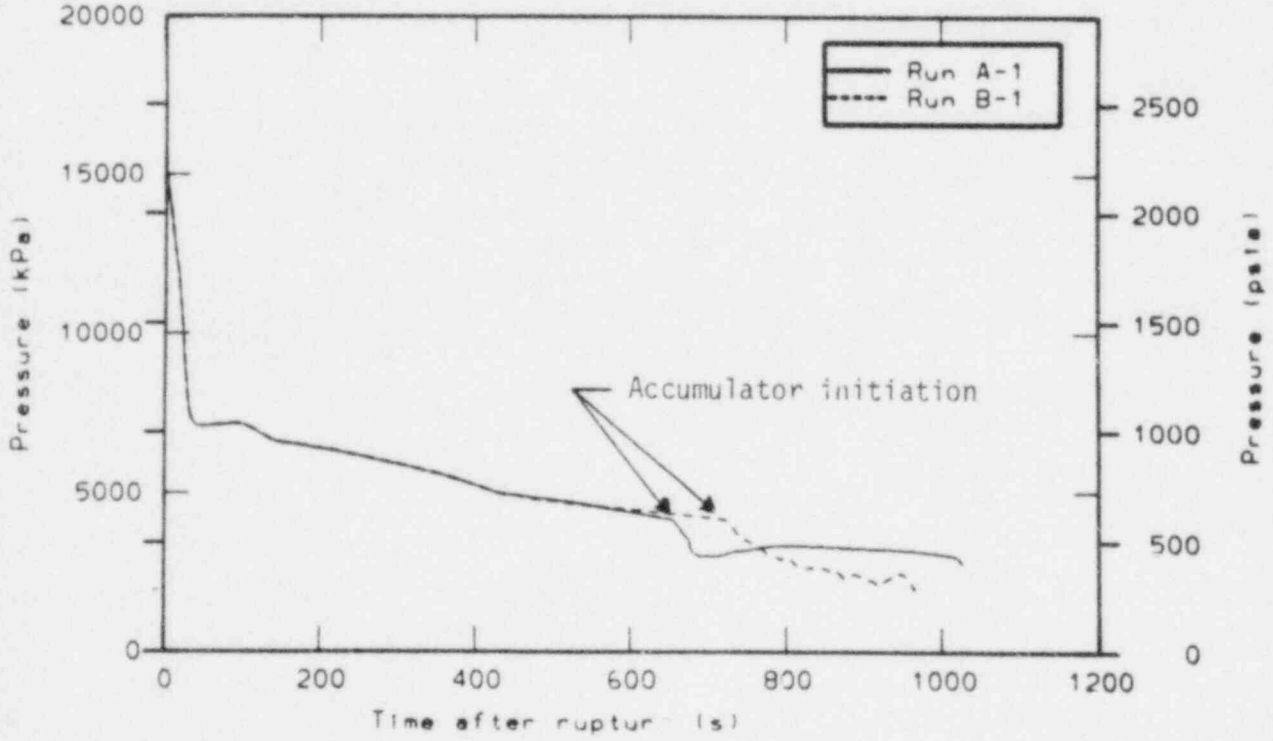

Figure 12. Upper plenum pressure vs. time for Runs A-1 and B-1.

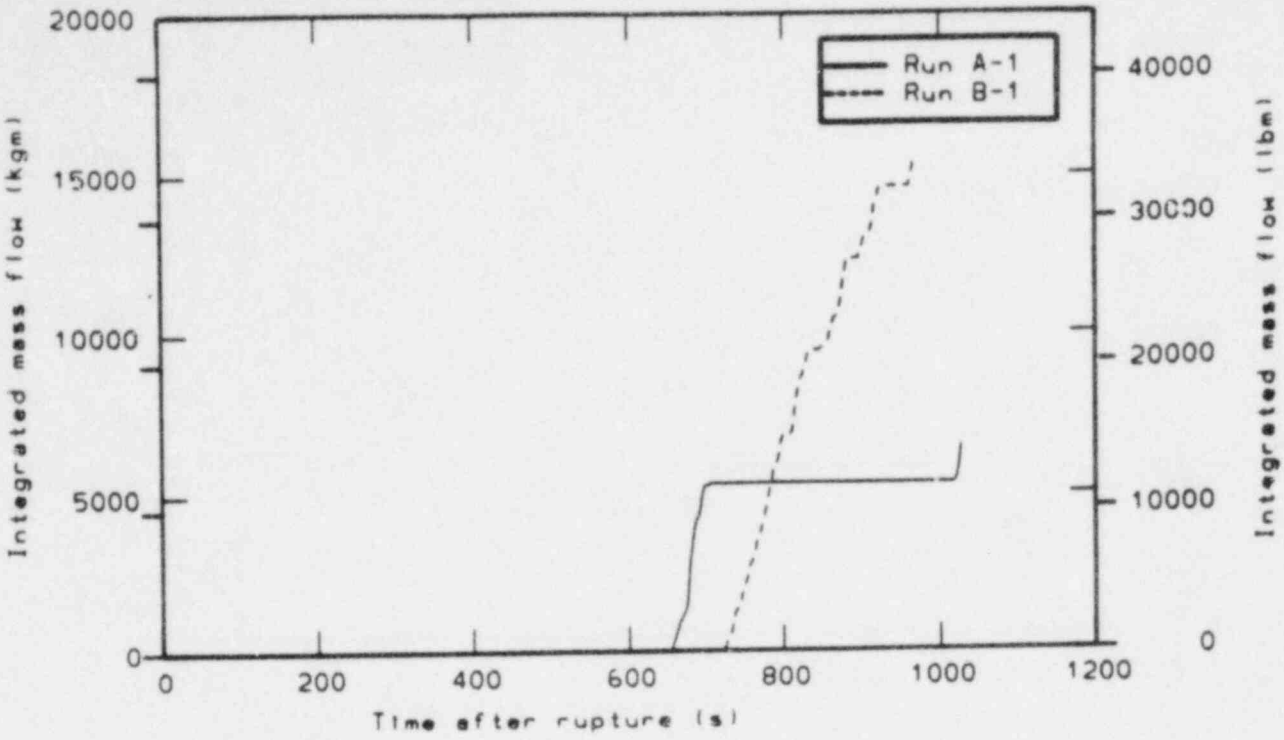

Figure 13. Integrated broken loop accumulator mass flow vs. time for Runs A-1 and 3-1.

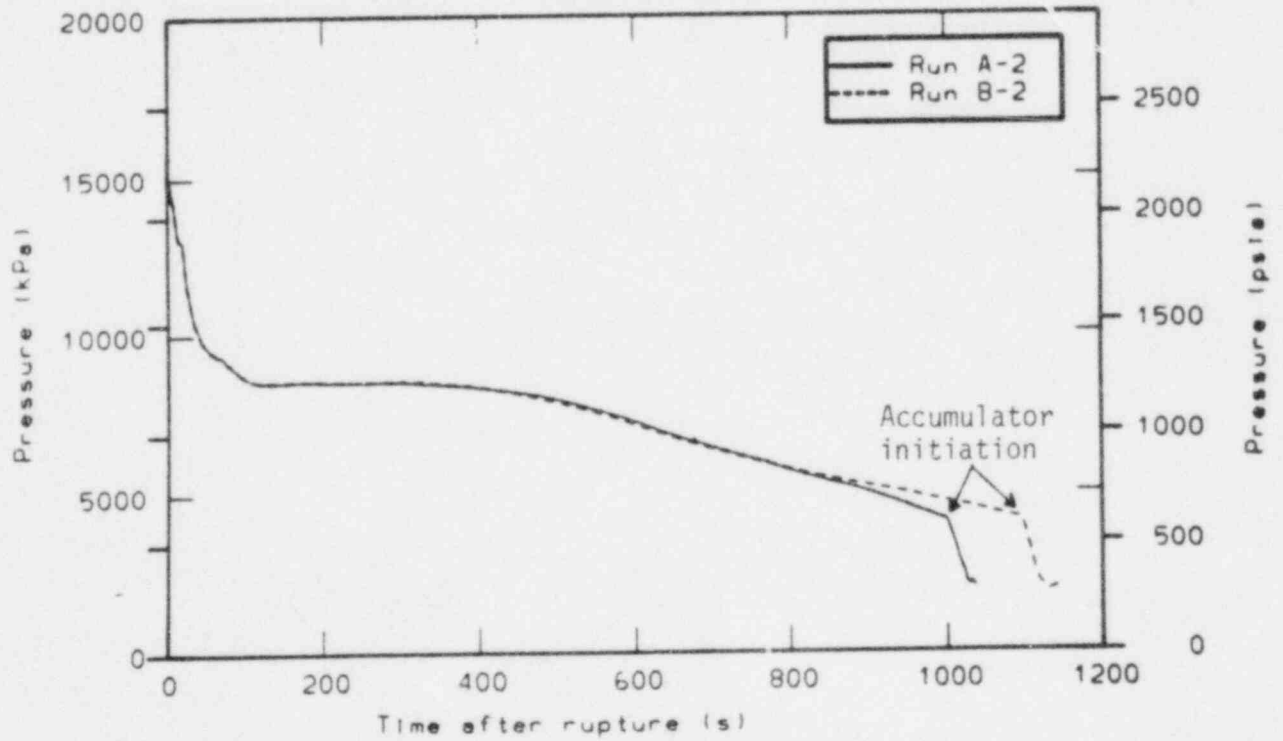

Figure 14. Upper plenum pressure vs. time for Runs A-2 and B-2.

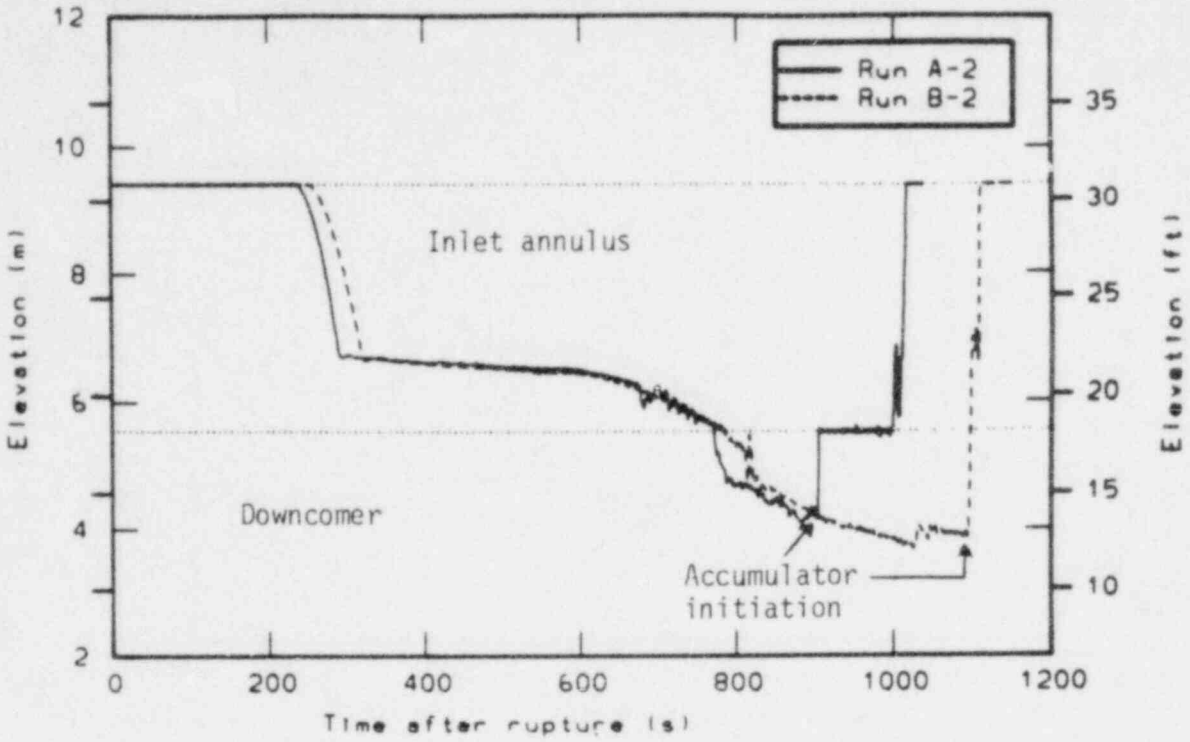

Figure 15. Downcomer and downcomer inlet annulus mixture levels vs. time for Runs A-2 and B-2.

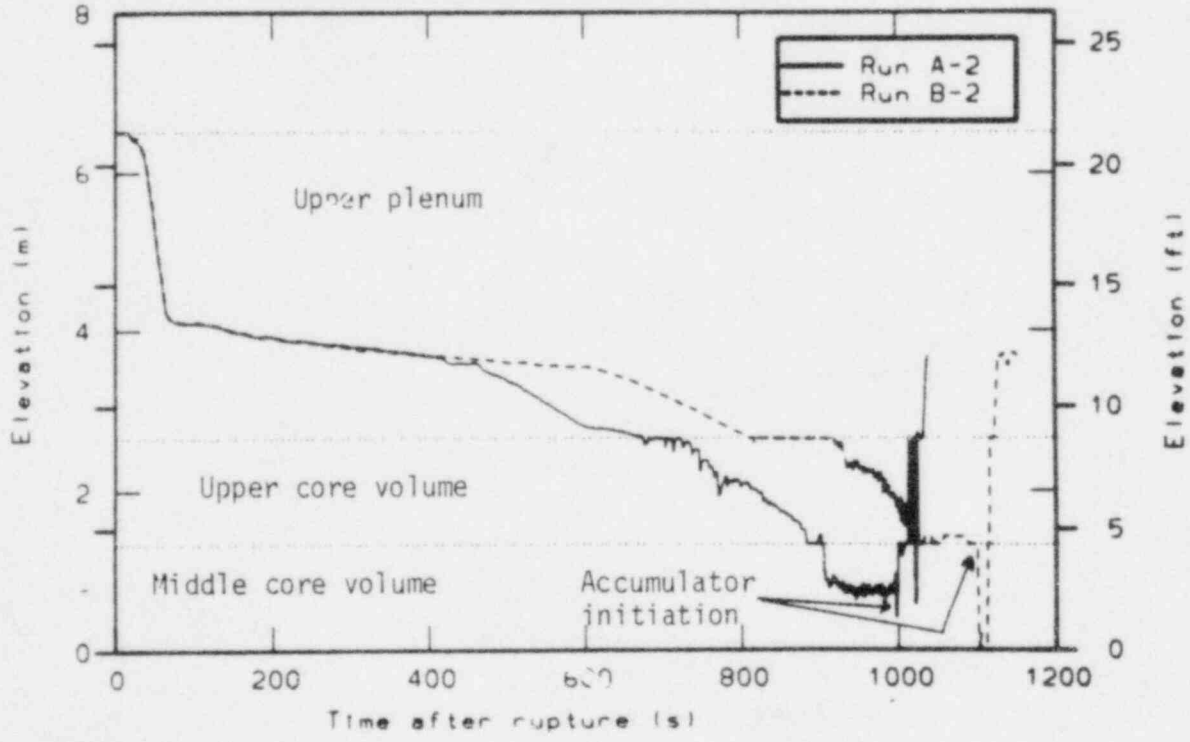

Figure 16. Upper plenum and core mixture levels vs. time for Runs A-2 and B-2.

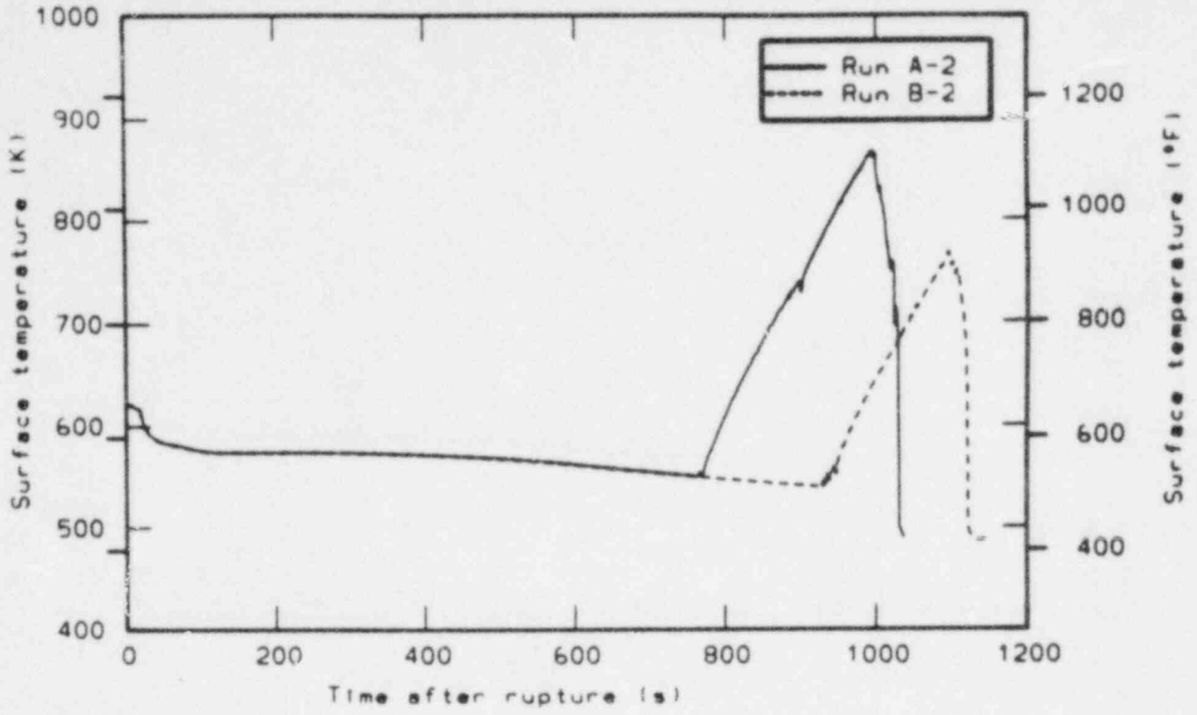

Figure 17. Fuel rod cladding surface temperature 3.0-3.7 m. above the core inlet vs. time for Runs A-2 and B-2.

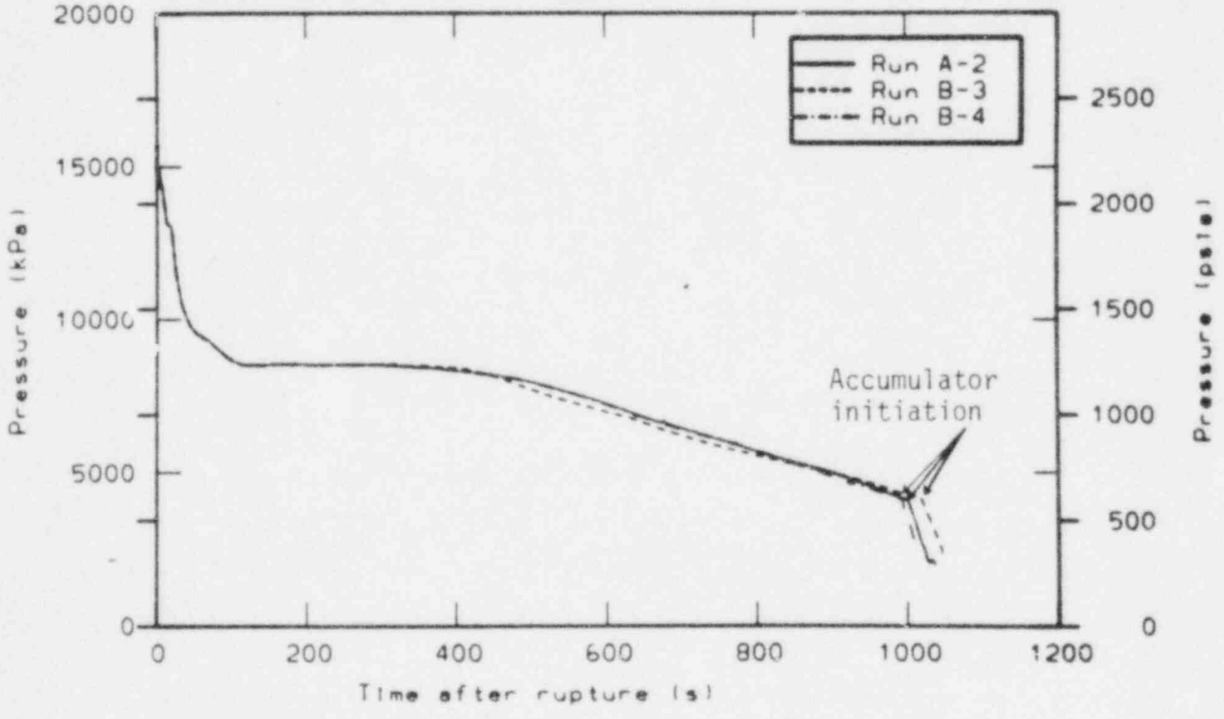

Figure 18. Upper plenum pressure vs. time for Runs A-2, B-3, and B-4.

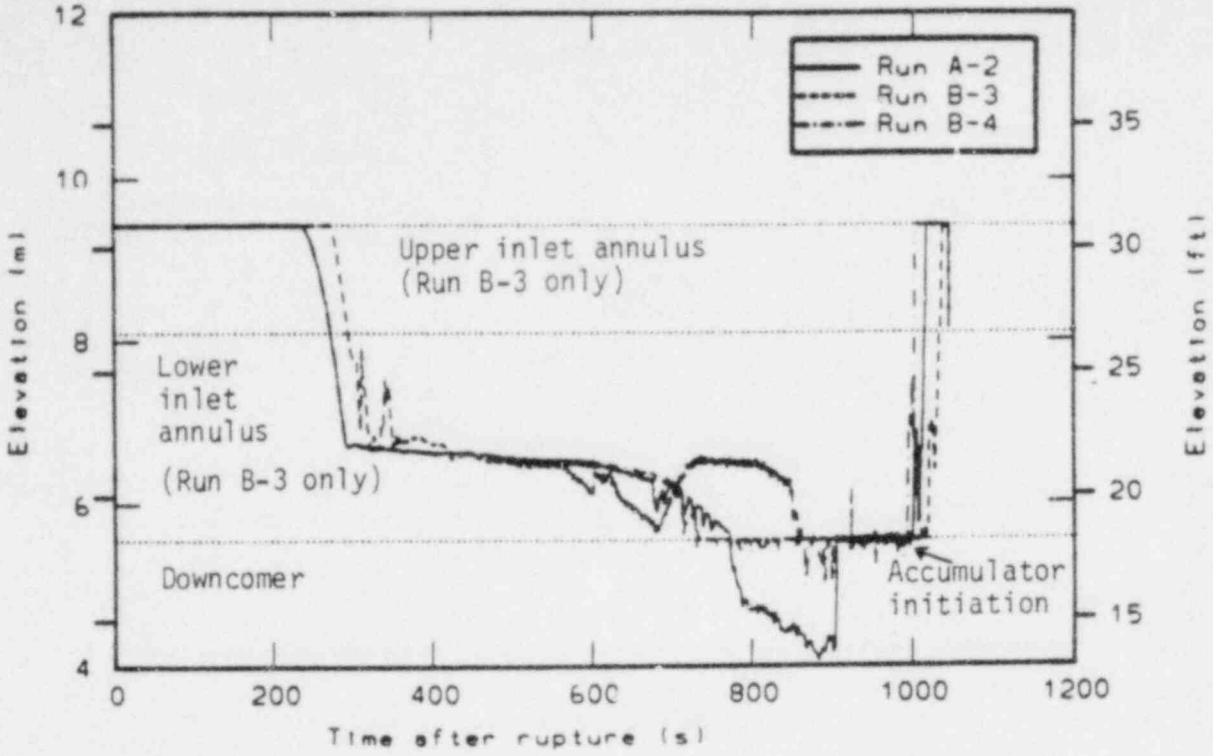

Figure 19. Downcomer and downcomer inlet annulus mixture levels vs. time for Runs A-2, B-3, and B-4.

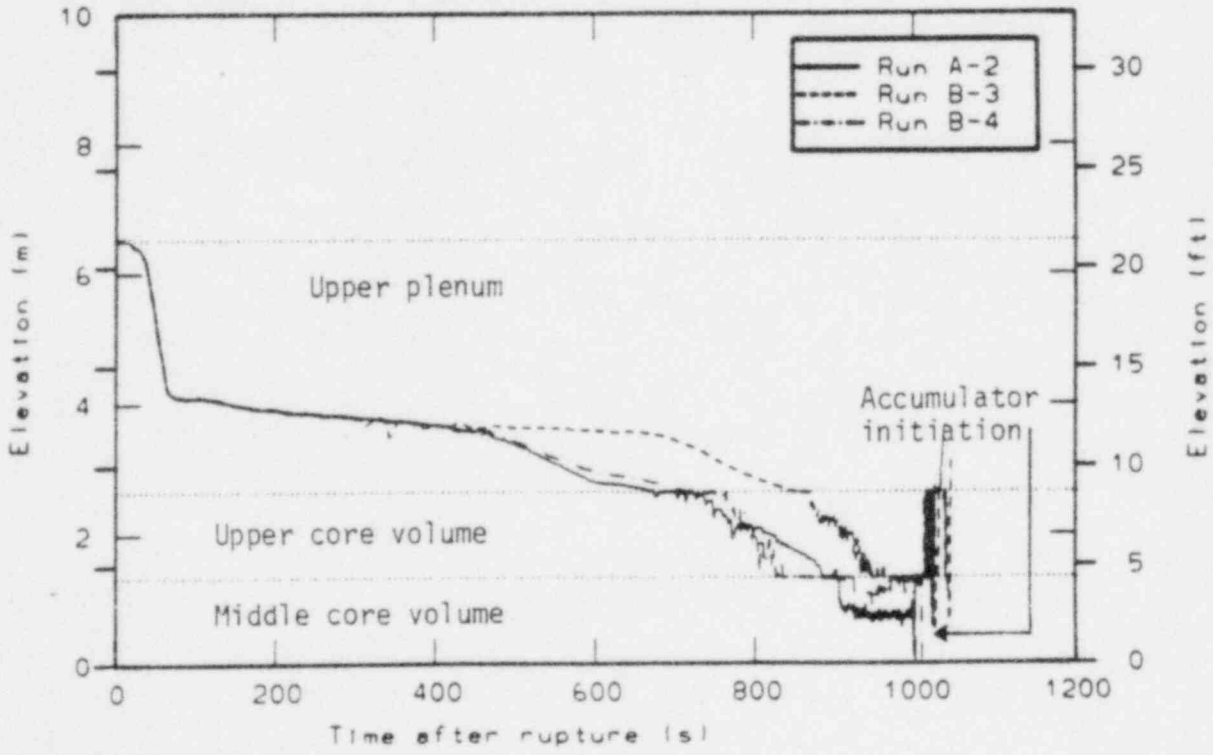

Figure 20. Upper plenum and core mixture levels vs. time for Runs A-2, B-3, and B-4.

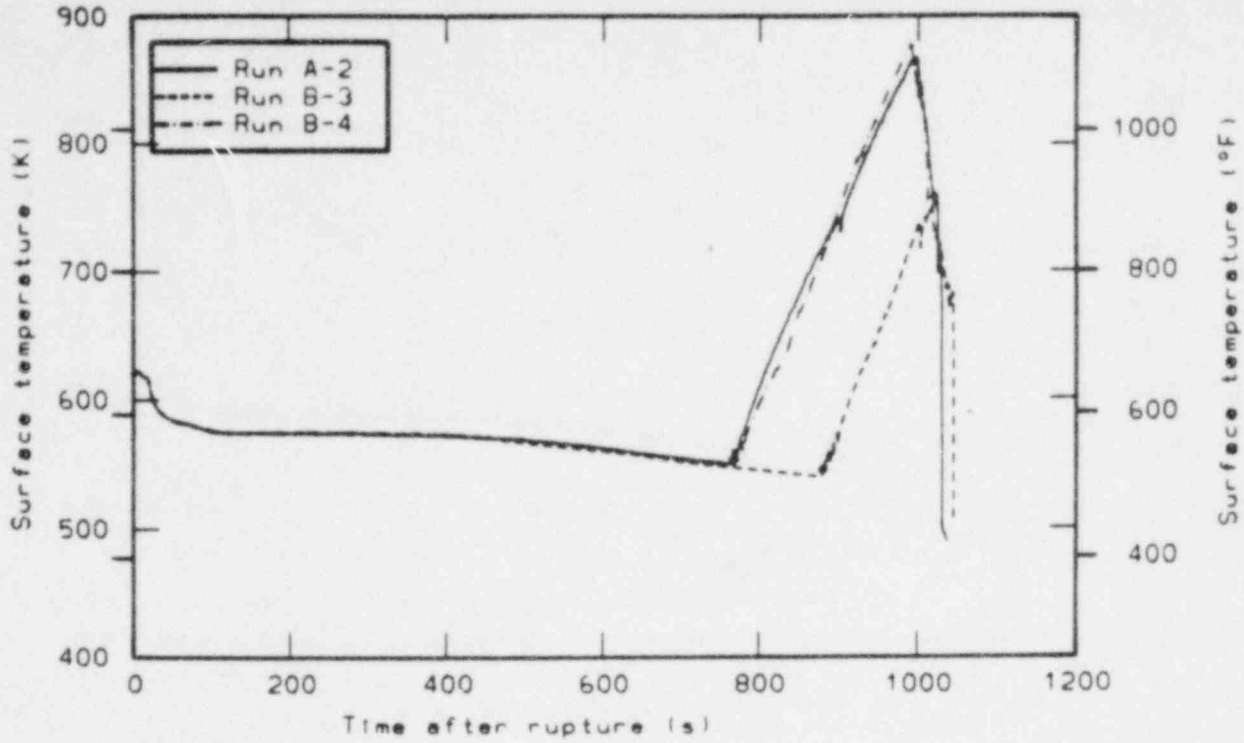

Figure 21. Fuel rod cladding surface temperature 3.0-3.7 m. above the core inlet vs. time for Runs A-2, B-3, and B-4.

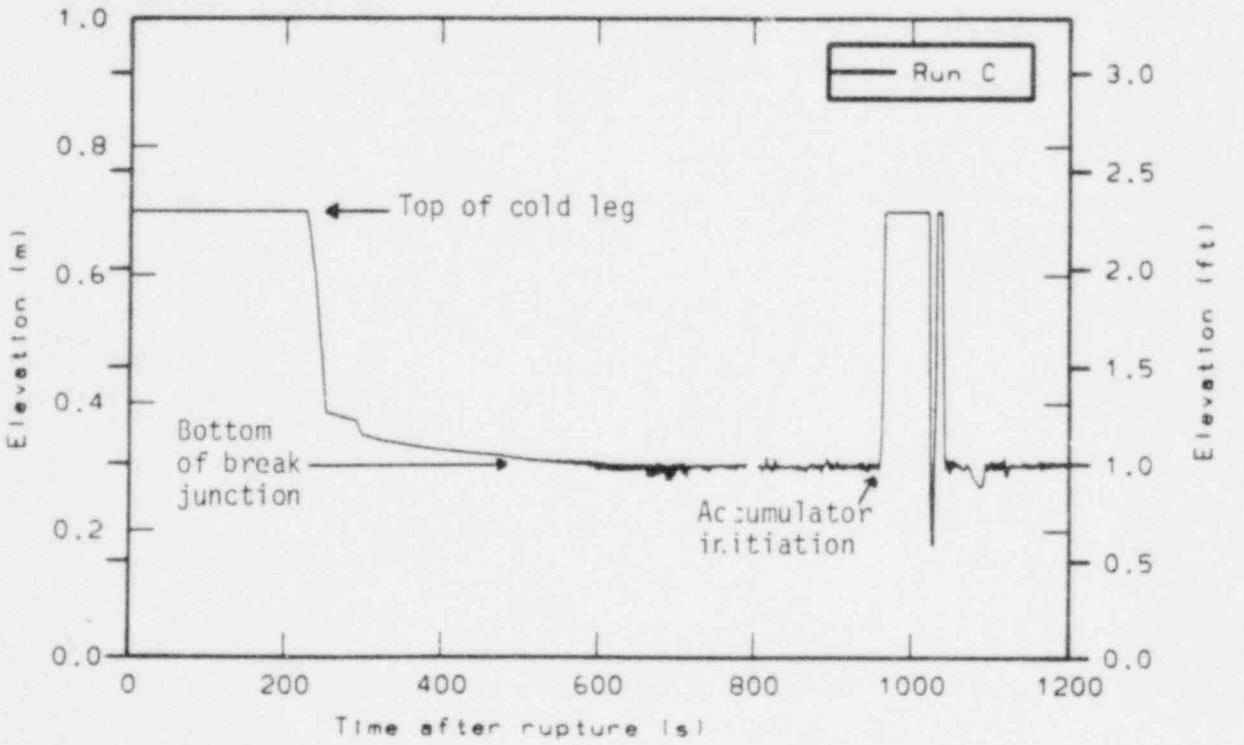

Figure 22. Broken loop cold leg mixture level vs. time for Run C.

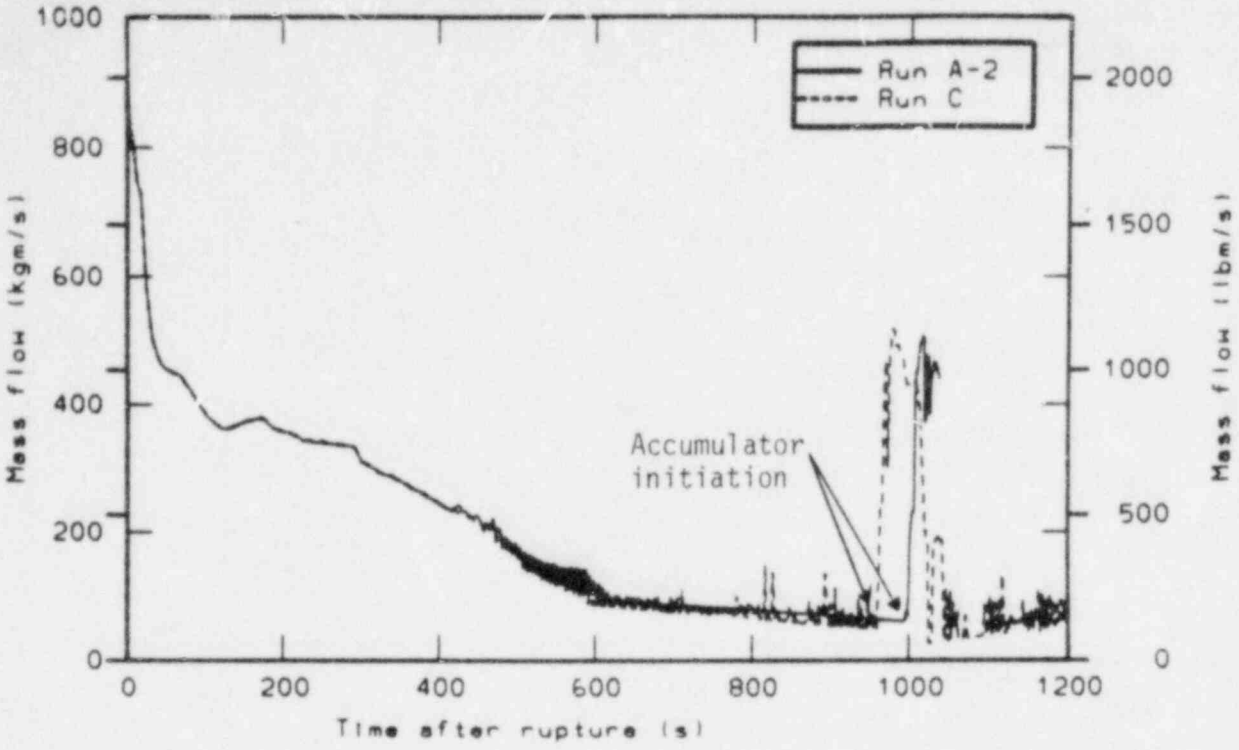

Figure 23. Break mass flow rate vs. time for Runs A-2 and C.

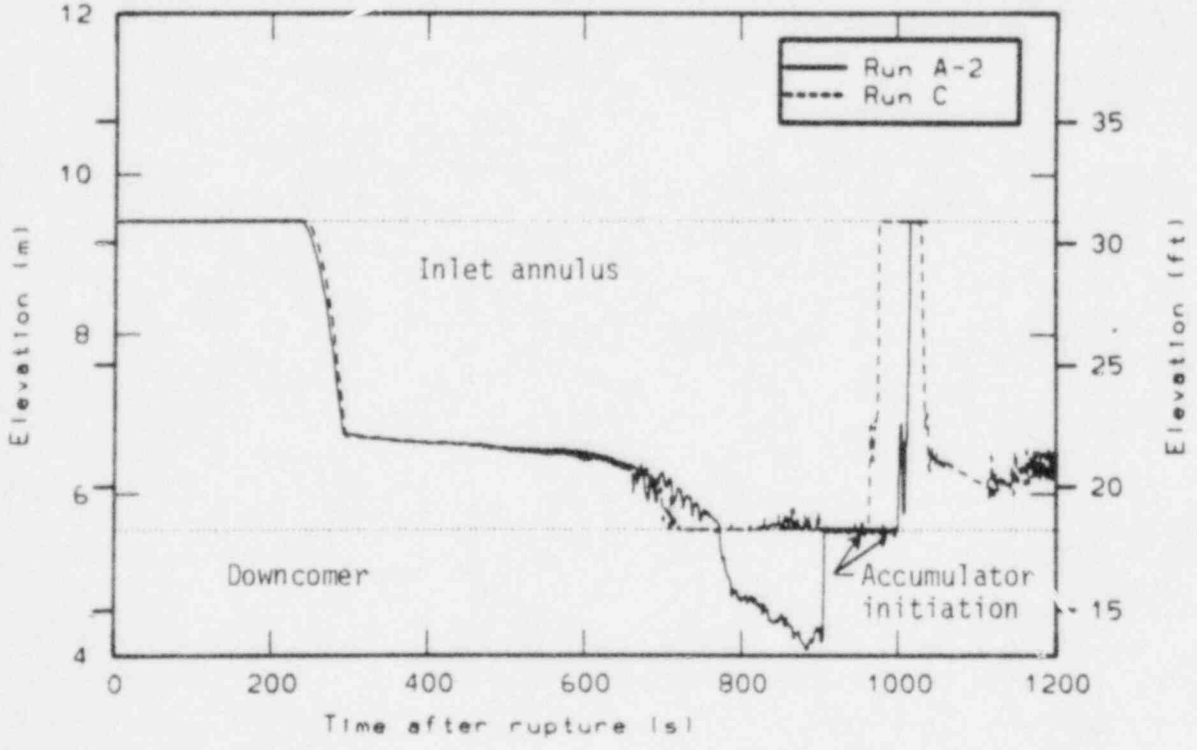

Figure 24. Downcomer and downcomer inlet annulus mixture levels vs. time for Runs A-2 and C.

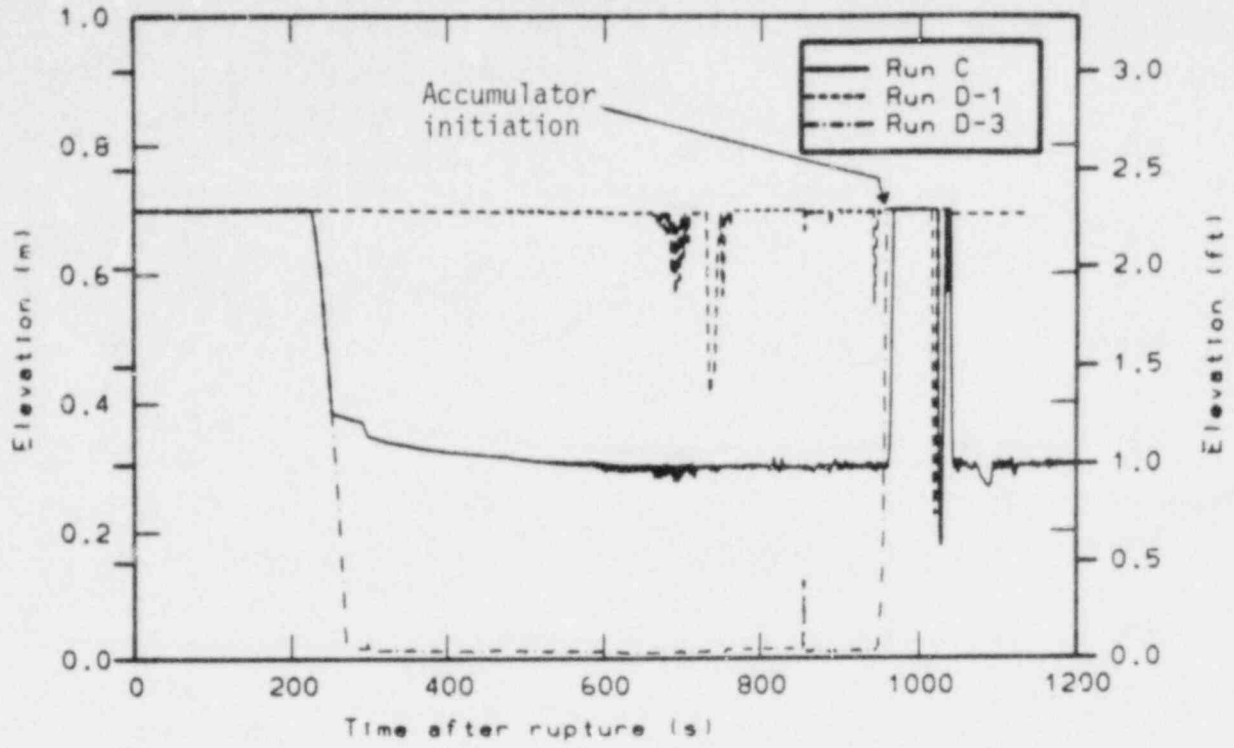

Figure 25. Broken loop cold leg mixture level vs. time for Runs C, D-1, and D-3.

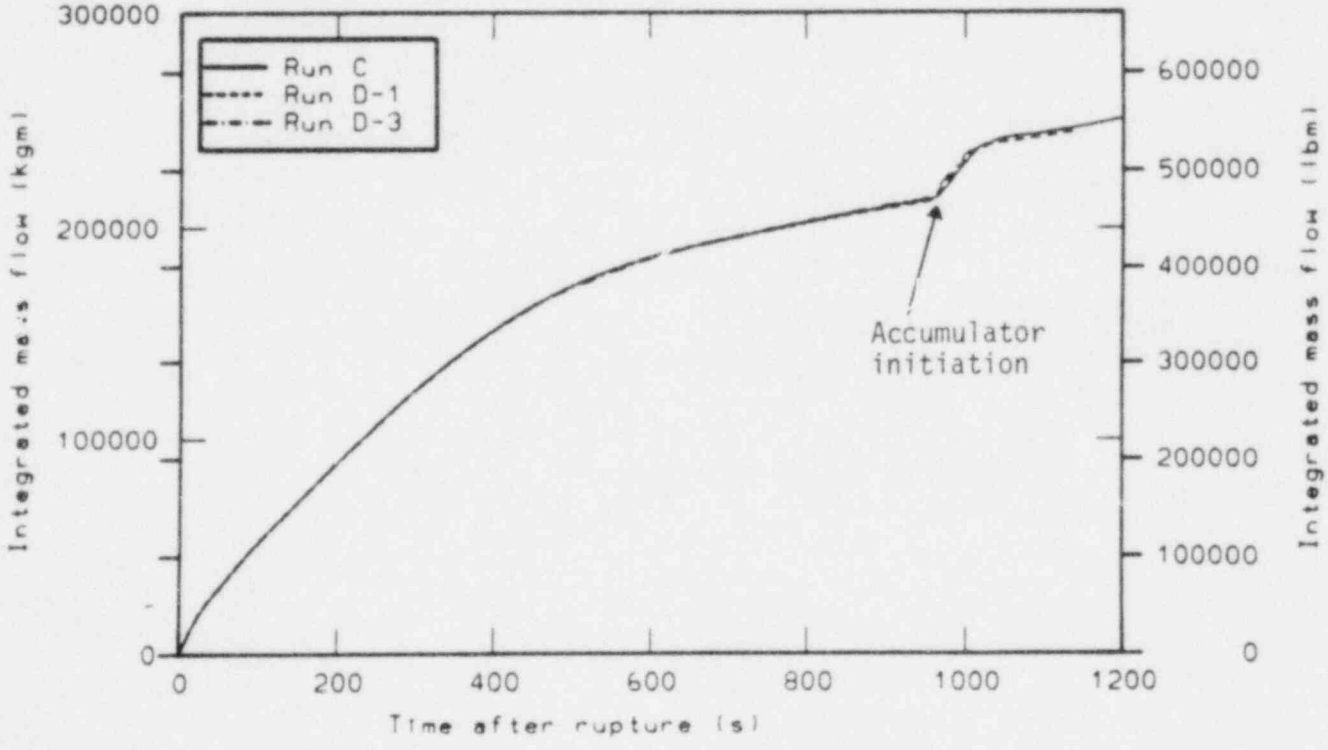

Figure 26. Integrated broken loop accumulator mass flow vs. time for Runs C, D-1, and D-3.

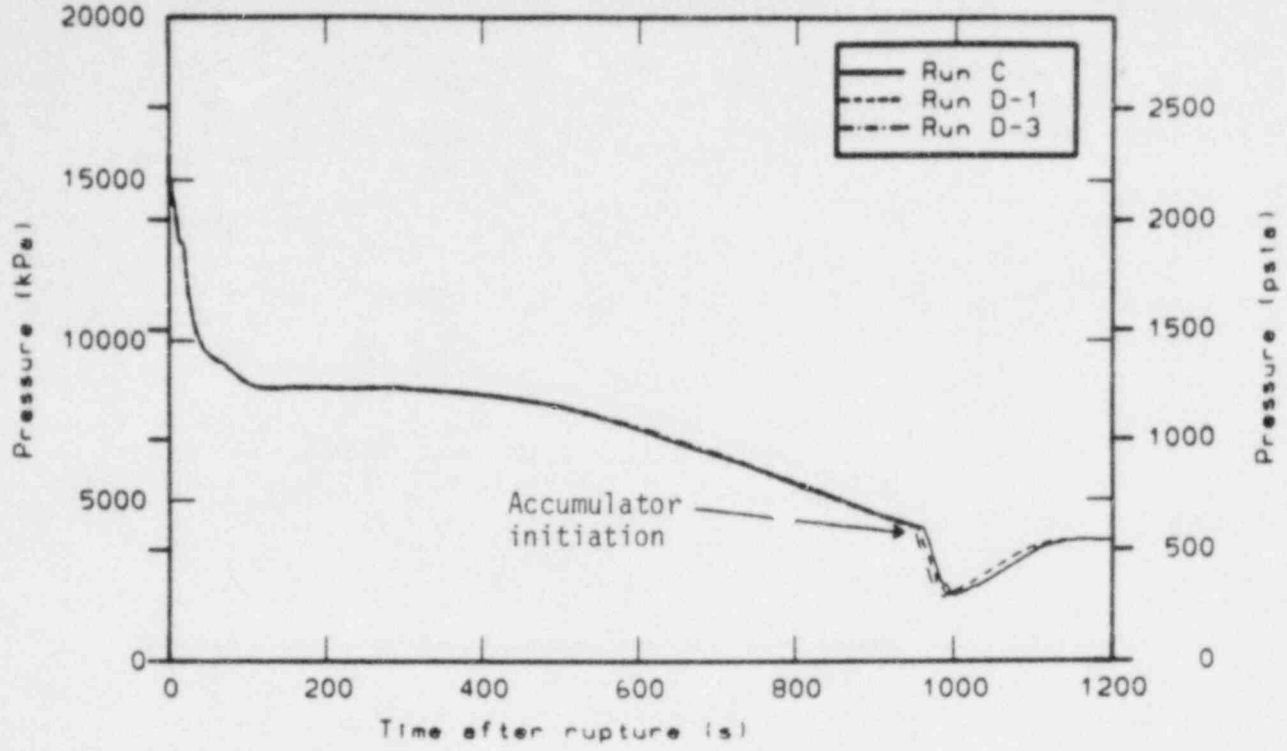

Figure 27. Upper plenum pressure vs. time for Runs C, D-1, and D-3.

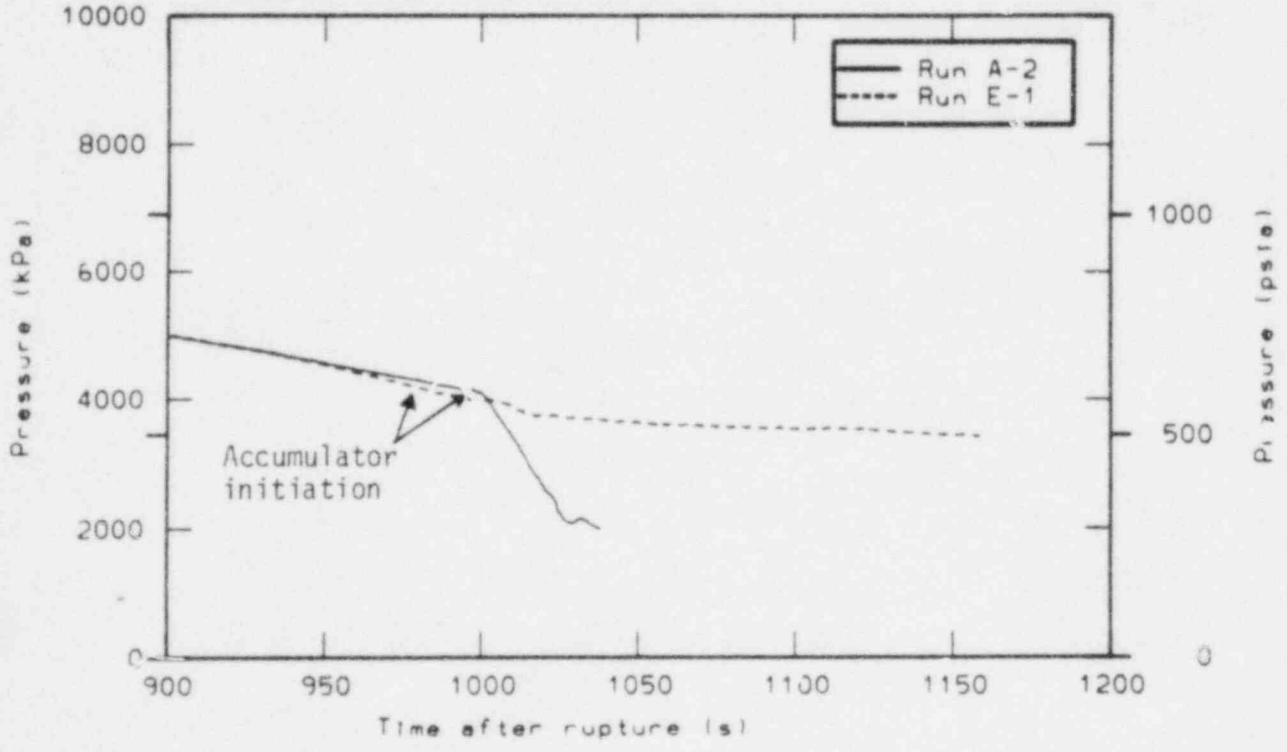

Figure 28. Upper plenum pressure vs. time for Runs A-2 and E-1.

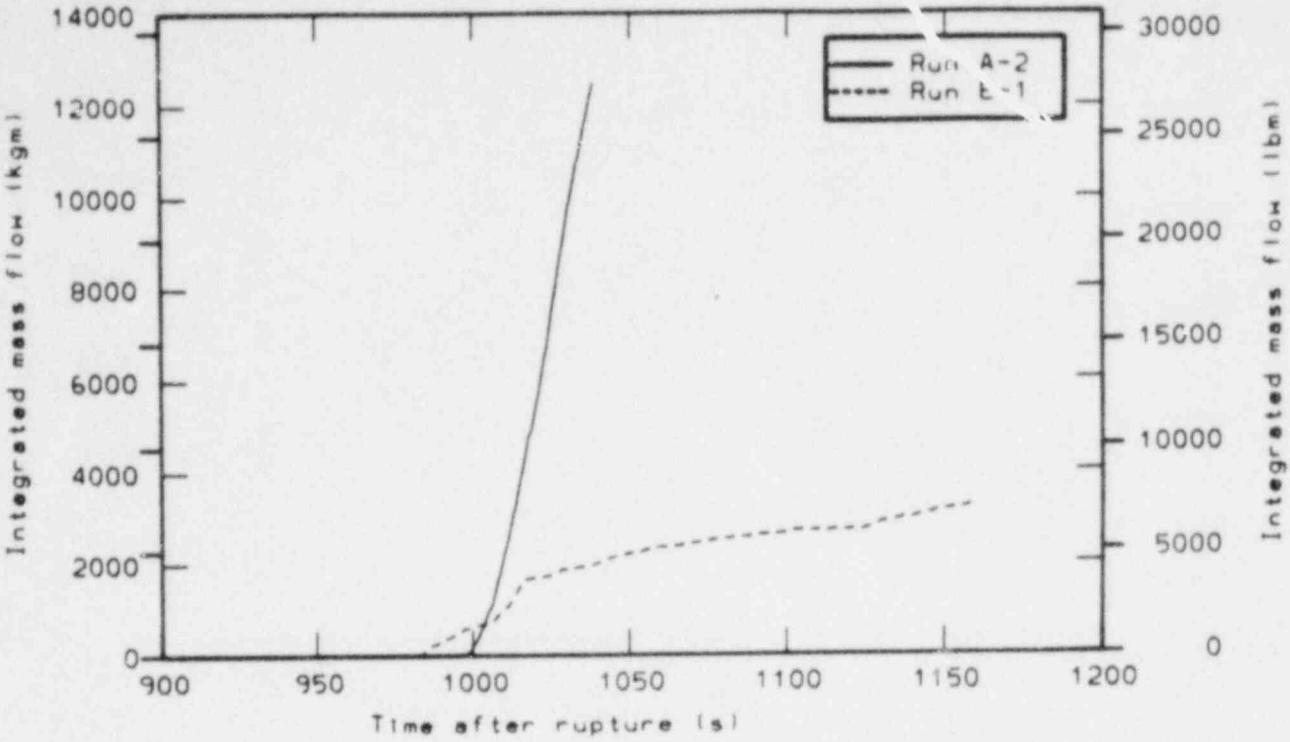

Figure 29. Integrated broken loop accumulator mass flow vs. time for Runs A-2 and E-1.

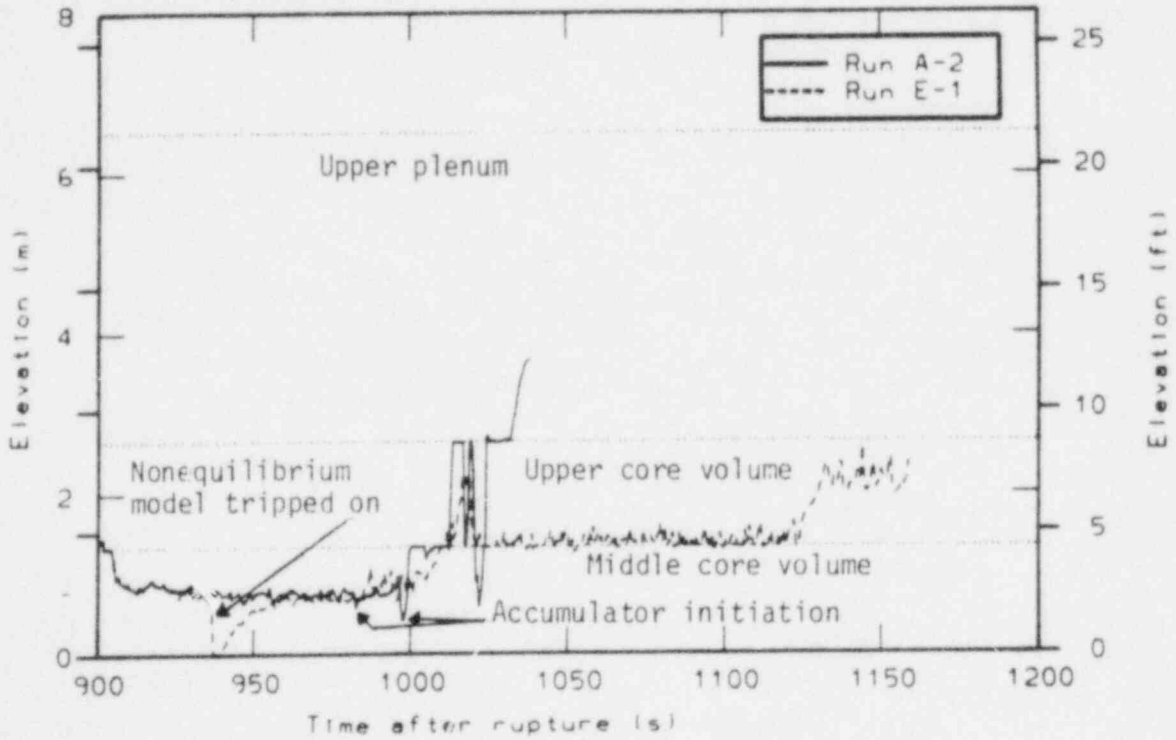

Figure 30. Upper plenum and core mixture levels vs. time for Runs A-2 and E-1.

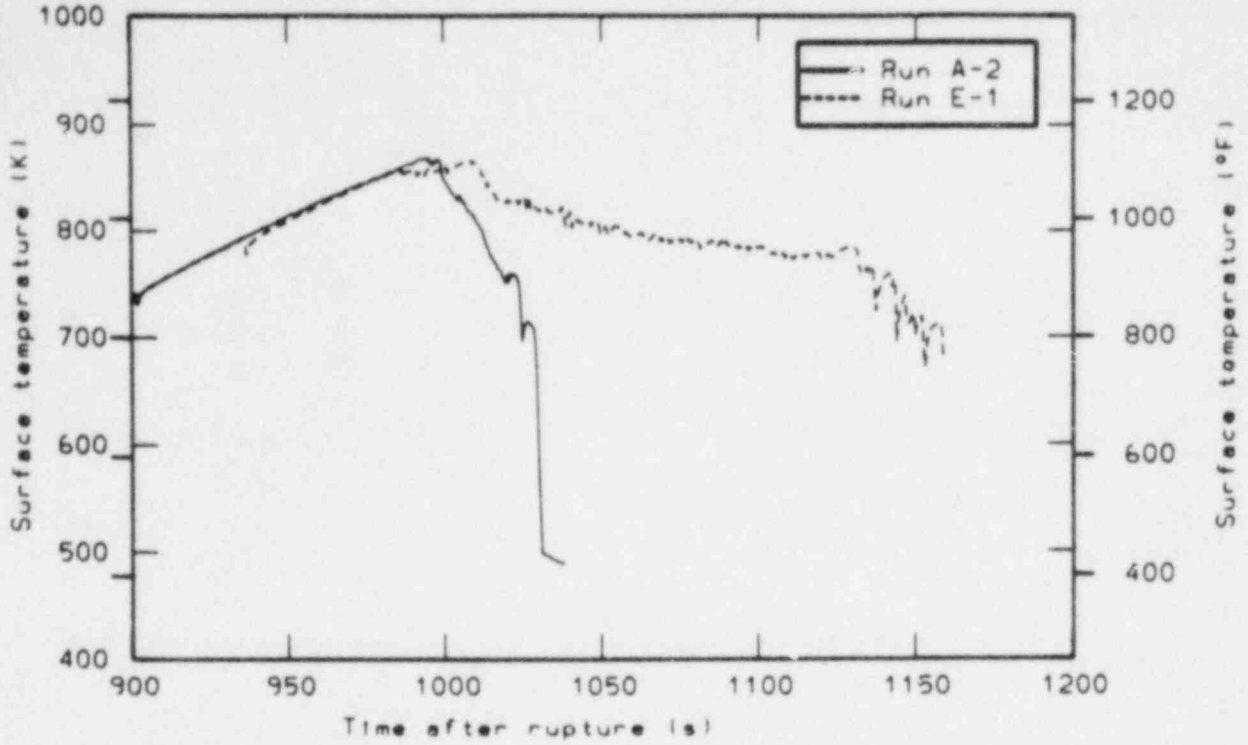

Figure 31. Fuel rod cladding surface temperature 3.0-3.7 m. above the core inlet vs. time for Runs A-2, and E-1.

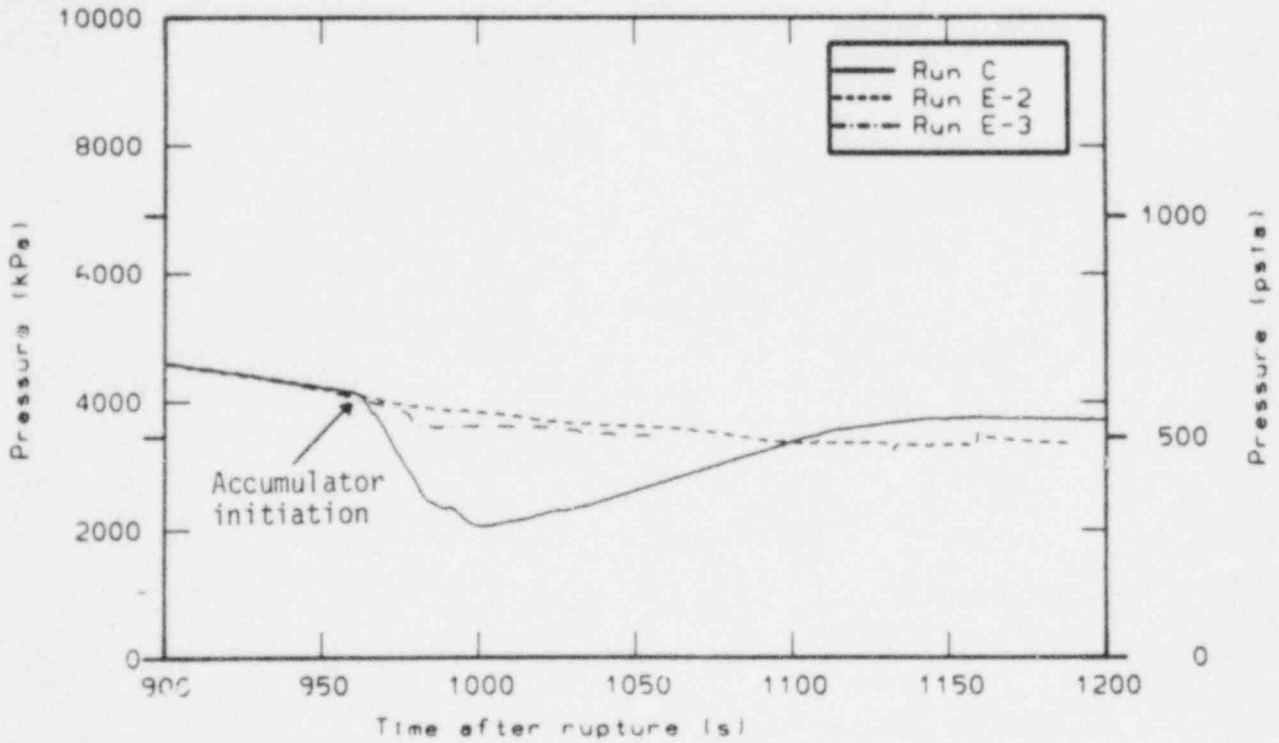

Figure 32. Upper plenum pressure vs. time for Run C, E-2, and E-3.

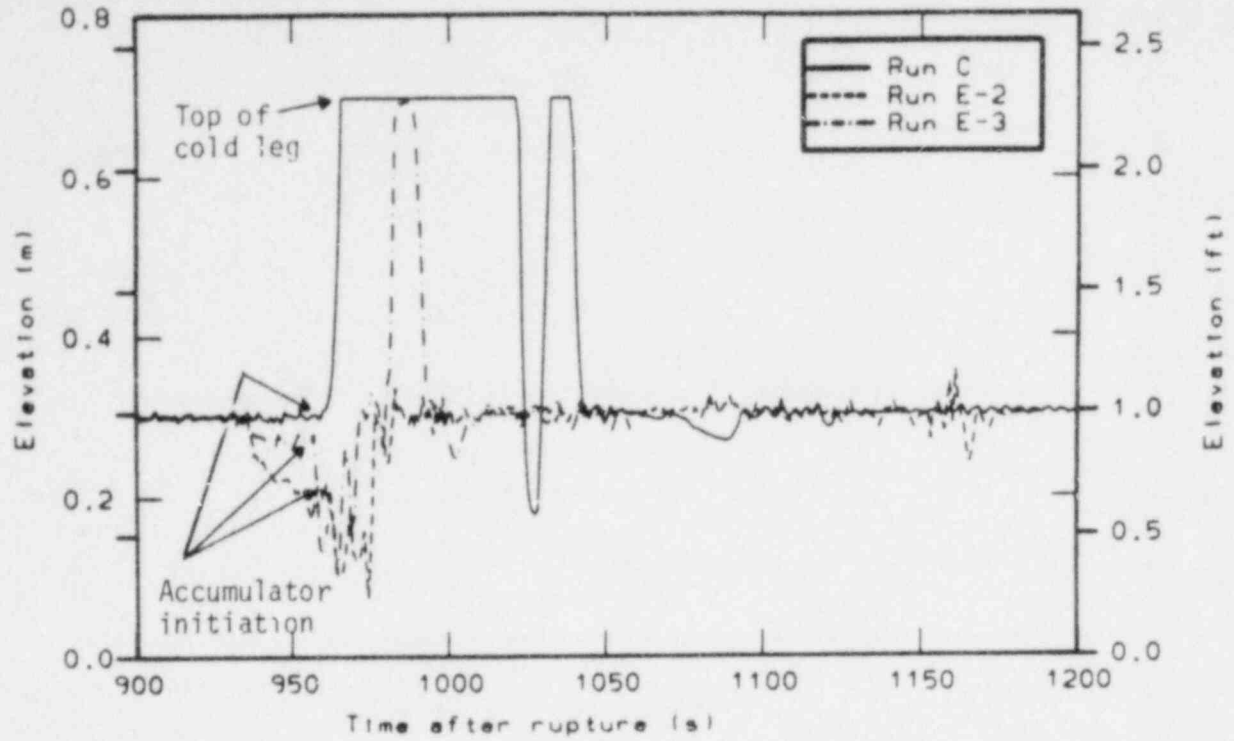

Figure 33. Broken loop cold leg mixture level vs. time for Runs C, E-2, and E-3.

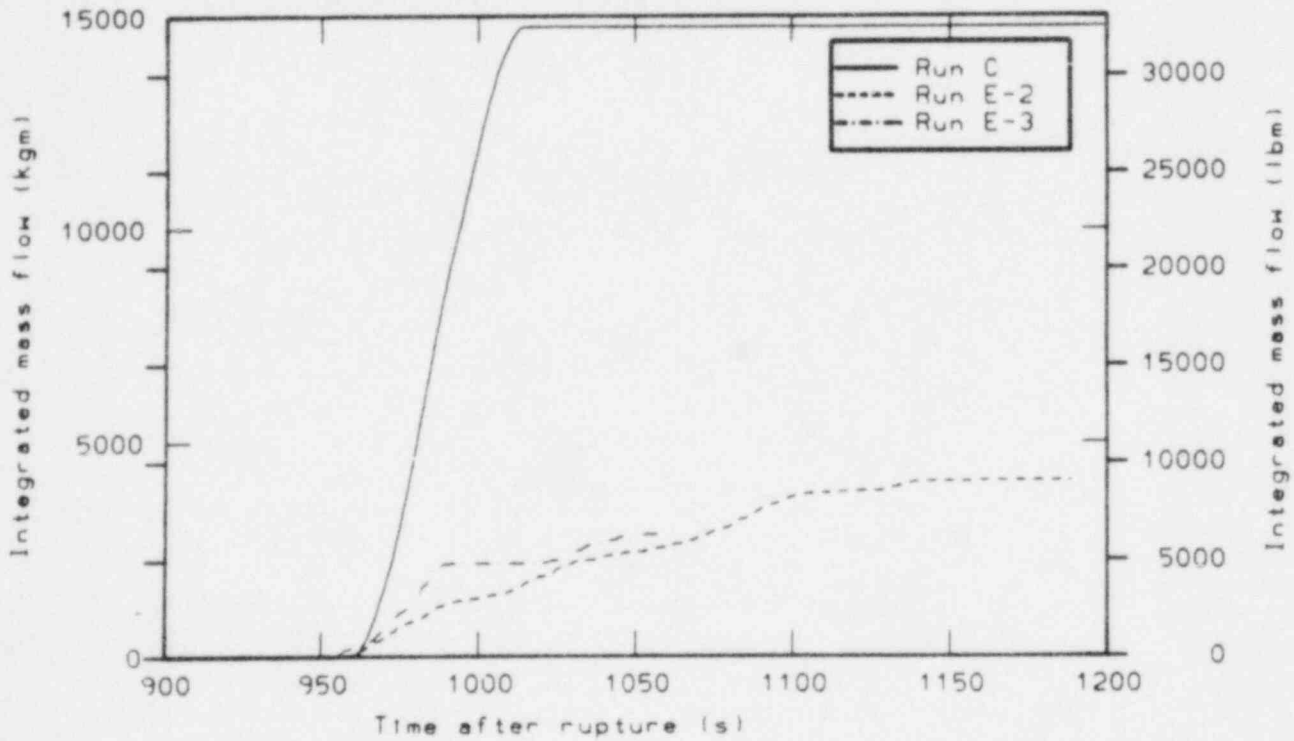

Figure 34. Integrated broken loop accumulator mass flow vs. time for Runs C, E-2, and E-3.

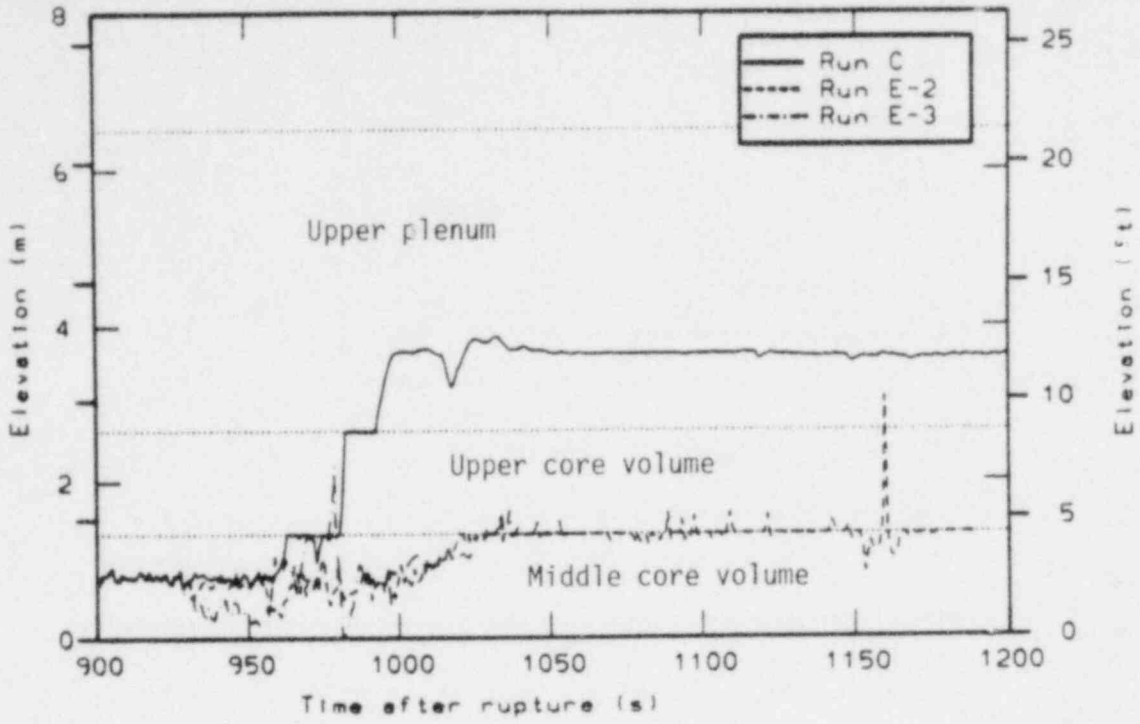

Figure 35. Upper plenum and core mixture levels vs. time for Runs C, E-2, and E-3.

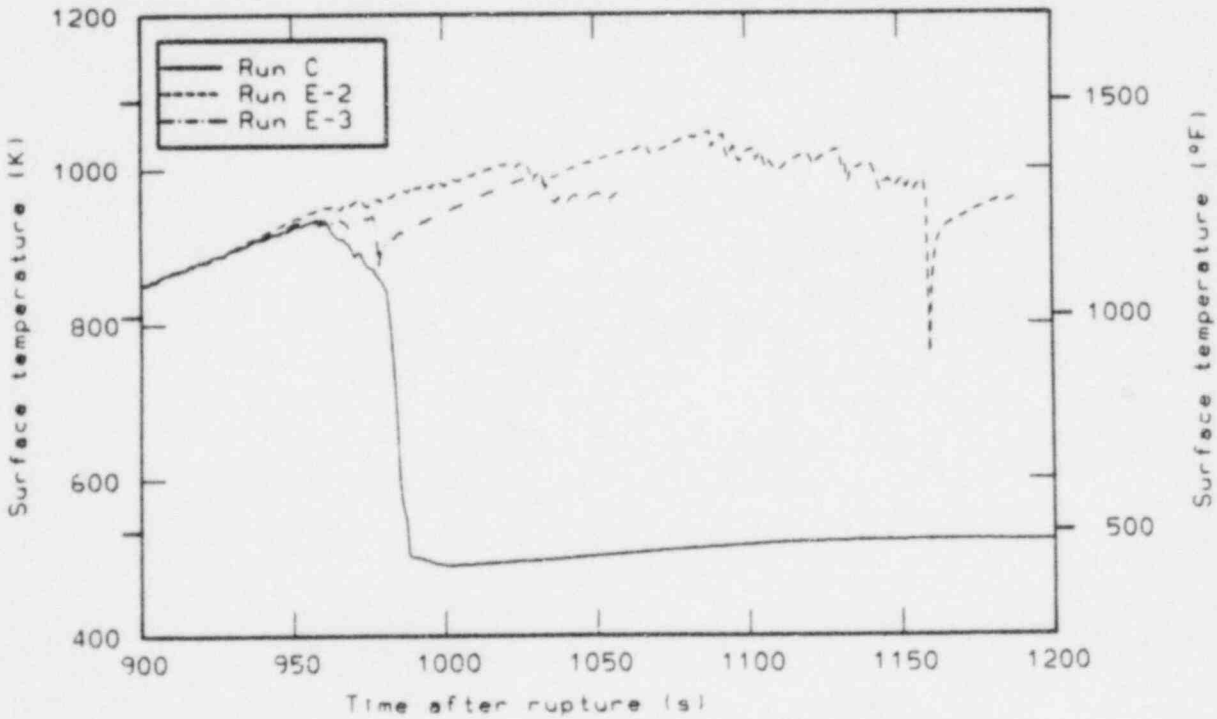

Figure 36. Fuel rod cladding surface temperature 3.0-3.7 m. above the core inlet vs. time for Runs C, E-2, and E-3.